Volume 4, Issue 3, 2026

Frontier in Medical & Health Research

ISSN: (e) 3007-1607 (p) 3007-1593

SYNTHESIS OF KNOEVENAGEL DERIVATIVES AND THEIR MOLECULAR DOCKING STUDIES FOR BLOOD CANCER

Ali Raza*

*Department of Chemistry, University of Sahiwal, Sahiwal, Pakistan

*alirazahussain960@gmail.com

DOI: https://doi.org/10.5281/zenodo.21974877

Keywords

Synthesis, Characterization, Antibacterial, Antifungal, Molecular Docking, Anti-Blood Cancer Potential.

Article History

Received: 20 January 2026
Accepted: 15 March 2026
Published: 29 March 2026

Corresponding Author: *
Ali Raza

Abstract

*Knoevenagel condensation, a carbon-carbon bonding process, produces bioactive chemicals. Knoevenagel derivatives made with aromatic aldehydes may treat leukemia and lymphoma. The structural and electronic properties of aromatic aldehydes and active methylene reagents enabled the creation of various α, β-unsaturated carbonyl compounds. Mass, IR, and 1H-NMR confirmed the changed derivatives' structure. Lab tests examined their antibacterial and antifungal properties. Six novel knoevenagel derivatives (**1a-6a**) were computationally evaluated and synthesised as potential SOD3 inhibitors for hematological malignancies. After rigorous molecular docking simulations (AutoDock Vina, exhaustiveness=16), compound 2a was the most potent candidate with a binding affinity of -4.953 kcal/mol and an optimal combination of hydrogen bonds with catalytic residues (ASP500, ASN487) and extensive hydrophobic interactions (LEU489, ILE369). Structure-activity analysis identified three key inhibitor factors: (1) hydrogen bonding with catalytic residues, (2) hydrophobic complementarity with ALA389 Despite multiple hydrogen bonds, compound **5a** performed poorly (-1.975 kcal/mol), emphasizing steric compatibility. Computational predictions indicate active site competition, allosteric modulation, and cysteine coordination-mediated redox interference. Our findings support the development of next-generation knoevenagel-based SOD3 inhibitors, with compound **2a** promising for blood cancer treatment.*

1. INTRODUCTION

This chapter is about the introduction of knoevenagel derivatives, and their basic concepts are discussed in a easy approach to understand the knoevenagel derivatives.

A breakdown in cell function that results in apoptosis and cell death is a hallmark of cancer, a hyperproliferative disease. It continues to be a global public health issue. Chemotherapy is a powerful tool for halting tumor growth and curing cancer. To supplement the present chemotherapy methods, new treatment options with a distinctive mechanism operation, outstanding effectiveness, decent pharmacological a suitable level histories, and less adverse impacts have to be developed [1].This has fuelled the researcher's society's NCE creation. The findings have revealed some intriguing reactions that are being studied to find the best medicines.

Knoevenagel condensation, a base-catalyzed aldol-type reaction, is a common method for creating C=C bonds in α, β-unsaturated molecules like ketones and carboxylic acids. Acidic solutions and other environmentally friendly catalysts like amino compounds in catalytic quantities help the process [2].

Creating carbon-carbon bonds is crucial for synthesizing α, β-unsaturated acids in modern chemistry. These acids are found in cosmetics, polymers, and pharmaceuticals (1). Most consider Emil Knoevenagel a pioneer for discovering in 1894 that formaldehyde could form a carbon-carbon bond with diethyl malonate. Emil Knoevenagel discovered that diethylamine catalysts produce bisadduct. To verify a similar

Frontier in Medical & Health Research
ISSN: (e) 3007-1607 (p) 3007-1593

carbon bonding process, Knoevenagel tested aromatic aldehydes and piperidine as catalysts in 1896. Some call Piperidine cyclic diethylamine. Biochemically, many aromatic aldehydes in current chemistry are intriguing. Lignin produces many aromatic aldehydes. Papermaking waste is rich in lignin. A "Knoevenagel-like way" to make aromatic aldehydes could give the pharmaceutical industry bio-based alternatives [3]. A common synthetic pathway reaction, the Knoevenagel condensation process is named after German scientist Emil Knoevenagel. An active hydrogen-containing molecule is nucleophistically included to a carbonyl group in this modified aldol condensation. Reactivity later dehydrates water and creates a conjugated enone, an alpha, beta-unsaturated carbonyl compound. Reaction conditions include active hydrogen: Consist of diethyl malonate, etc. Structures with nitro groups (e.g., nitromethane) or other electron-withdrawing substituents stabilize enolate ion. Use a moderate base to deprotonate the enolate ion and avoid harsher bases to prevent carbonyl reactant self-condensation. For maximum reaction and minimum side reactions, a weakly basic amine is used [4].

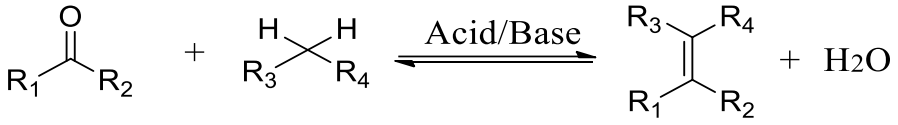

R_1= Alkyl, Aryl, H
R_2 =Alkyl, Aryl, H
R_3=CN, COMe, COOMe, COOEt, COOH
R_4= CN, COMe, COOMe, COOEt, COOH

Figure 1.1: Scheme for the synthesis of knoevenagel derivatives

1.1 The Mechanism of Knoevenagel condensation reaction

Three main phases define the mechanism of the Knoevenagel reaction: (i) deprotonation of the active methylene molecule by a base; (ii) nucleophilic attack on the carbonyl compound; and (iii) elimination of water to generate the α,β-unsaturated product. The response's amino catalysis is monitored by the mechanistic data, and special mechanisms have been suggested based on the response's bottom hire. This method claims that tertiary amines are important since they help form a β-hydroxy-dicarbonyl molecule. Usually, the Knoevenagel condensation reaction works by converting the one or two amine into an iminium ion, which is known to become the condensed molecule after losing water during dehydration. Acting as a strong electron-taker, electronegativity on the active methylene group is necessary for the enolate formation after deprotonation is done on moderate conditions. However, having these products tells us the way is well built. In acid-catalyzed Knoevenagel condensation, both the nucleophilic addition and the dehydration steps take place in sequence as you see in Scheme 1[5].

Many researchers have examined variations of Knoevenagel condensation called Henry, Doebner, and Verley, all having different substrates, products, and catalysts involved. Even though the starting substrates are very similar to the traditional reaction, the importance of these reactions increases due to their results and how reactive the product can be. Because of Louis Henry's work, Belgian scientist Louis Henry modified the Knoevenagel reaction and introduced Henry's response in 1895. When a nitroalkane reacts with a carbonyl group like ketone or aldehyde, while a base is present, β-nitro alcohols are made. This reaction, called the Knoevenagel-Doebner reaction, got its name after Oscar Doebner's breakthrough. With the help of malonic acid, the method forms α, β-unsaturated carboxylic acids that are then identified by removing one carboxylic group. For the traditional Knoevenagel reaction, β-alanine, not piperidine, is used as a co-catalyst in what is called the Verley variation. Albert Verley, the one who found the new mutant creature, is honored with this creature's name [3].

Volume 4, Issue 3, 2026

Frontier in Medical & Health Research

ISSN: (e) 3007-1607 (p) 3007-1593

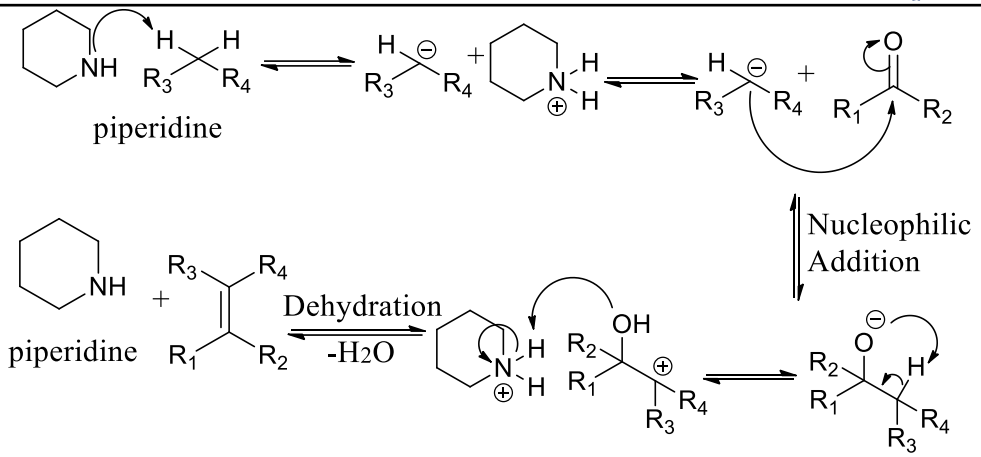

Figure 1.2: Knoevenagel Derivatives and their mechanism

1.2 Reactions of Knoevenagel Pharmaceutical Significance

Knoevenagel condensation is an important synthetic method for the manufacture of α,β-unsaturated carbonyl compounds which are used in polymers, resins, dyes, agrochemicals, and pharmaceuticals. The products are also essential intermediates in the synthesis of heterocyclic compounds via the reactions of Gewald, Feist-Benary and Hantzsch syntheses. Several Knoevenagel derivatives have exhibited potential antiviral, antitubercular, antiparkinsonian and anticancer activity [6-8]. Recent advances include ionic liquids, nanostructured and organic catalysts, Lewis acids and microreactor systems to improve reaction efficiency. Microreactors have quick heat and mass transfer characteristics which enhance conversion, selectivity, yield and safety, notably for oxidation, hydrogenation and acid or base catalysed condensation reactions [10]. In accordance with the principles of green chemistry, the reduction of hazardous solvents, energy consumption, waste and difficult to recover catalysts have become more and more significant . The conventional Knoevenagel reactions often need toxic organic solvents, lengthy reaction times, high temperatures and complex work-up procedures, therefore stimulating the development of aqueous, solvent-free, ionic-liquid, microwave-assisted and recyclable catalytic systems [11–15]. They can be efficient for synthesis and have a minimal environmental effect, although scalability, catalyst recovery and energy requirements may still be of issue. In the present study, aromatic and heterocyclic aldehydes have been reacted with malononitrile under the selected catalytic conditions and the Knoevenagel derivatives were produced by filtration in good yields confirming the success of the used technique [16, 17].

2. LITERATURE REVIEW

In this chapter, we will discuss the review of literature on the basis of previous work related to our knoevenagel derivatives. The history about knoevenagel derivatives is presented in an elaborated and year wise work.

2.1 Theoretical Background

According to Koen van Beurden et al., organic chemistry has focused on carbon–carbon bond formation for over 250 years to produce important molecules in industry and medicine. Knoevenagel condensation uses nitrogen-based catalysts like amines and ammonium salts to produce structurally diverse intermediates that affect reaction speeds. Despite its under appreciation in chemical studies, quantitative assessments like e-aspect calculations have been used to evaluate these catalytic techniques, highlighting Knoevenagel chemistry's importance in modern synthetic and green chemistry. [3].Baijie Xu et al. found that enhancing the Knoevenagel condensation reaction with the latest hybrid catalysts is likely essential for practical applications. The organophosphonates-functionalized polyoxomolybdates were synthesised. For the gram-scale Knoevenagel condensation of benzaldehyde with ethyl cyanoacetate, is highly catalytic. Compound 1 yields 98% and has a high TONNE price (1960), outperforming compounds 2 and 3. This applies

Frontier in Medical & Health Research
ISSN: (e) 3007-1607 (p) 3007-1593

notably under gold standards. According to sources, TONNE costs substantially more than the planned catalysts. Lewis acidic and basic regions in the catalyst may improve catalytic performance. Based on substrate screening and recyclability experiments, 1 is enzymatically versatile and potentially reusable [18].

Balasubramanian Sakthivel et al. observed that element analysis, X-ray diffraction, and infrared spectroscopy show that chitosan enhances carbonyl compound and malononitrile Knoevenagel condensation in moderate Chitosan was improved for numerous substrates with benzaldehyde and malononitrile. Chitosan retained catalytic activity in four leaching and reuse studies [19]. Tokala et al. propose Knoevenagel condensation as a greener method for producing α, β-unsaturated ketones and carboxylic acids employing carbonyl functionalities and active methylenes. Multiple multicomponent reactions show this reaction creates intriguing biological compounds. The exceptional reaction on aromatic pharmacophores and chemically active methylene molecules generated substances. Understand this mechanism to boost pharma research. Most reactions targeting genetic material, microscopic Topo-I/II tubules, and regulators with micro to very low anticancer activity were created. Knoevenagel condensation developed cancer-targeted compounds over six years. Study shows it work. Coumadin's bend. Rajesh H et al. say Knoevenagel condensation coumarin synthesis is essential in medicinal and synthetic organic chemistry. Coumadin's bend. Thus, several methods have been developed to synthesize this essential chemical family. Methods with toxic catalysts, long reaction times, low yields, purity, and byproducts exist. Some approaches are unsafe and ineffectual. Many researchers have developed gentle, effective, and eco-friendly Knoevenagel condensation methods to synthesize pure, high-yield coumarin derivatives [20]. Ranise et al. made isolable tertiary N-methyleniminium chloride compounds 3 and 4 and benzoic acid in one pot using benzoyl chloride–N, N-dimethylformamide complexes with ethylenethiourea (1) and ethylene urea (2). Organic energetic methylene reagents (X–CH2–E) or 5 with tertiary amine (1.5 equity) decomposed salts 3 and 4 into N-formyl products 6 and 7, yielding two α, β-unsaturated compounds in low to high yields (Guide Stereo selectivity and 3–4 formation. Knoevenagel precipitation forms carbon molecular bonds in organic chemistry research, according to David Esteban Quintero Jimenez et al. Intermediates can undergo many chemical reactions, hence organic synthesis uses most molecules. Microwaves are needed for Kneevenagel adduct [21]. Almuzaini promotes plastic, calcium antagonist, medical, cosmetic, and scent Knoevenagel condensation. This employs organic solvents. First, Knoevenagel uses ammonia bases, salts, and amines. Zeolites, aluminium oxide, and alkali-containing MCM-41 catalyze it. Fresh Knoevenagel condensation made greener, safer chemistry. Research shows that deep-eutectic solutions (DES) are safe, affordable two- to three-solid combinations. Deep eutectic solvents (DES) generated hydrogen bonding between safe solids, making this reaction successful. DES is cheap, safe, and reusable. Rapid reactions yielded well. A deep eutectic solvent and catalyst study of Knoevenagel condensation. The effect of compound substitution on reactive methylene derivative reaction output is being studied [22].To find E and Z stereoisomers, specialists divide molecules into 3 and 6. Pregnenolone and 3-oxo-3-phenylpro-panenitrile yielded Knoevenagel condensed compounds, according to Rafat M. Mohareb e To assess cytotoxicity with healthy and cancer cells, researchers employed chemically altered products. Major cancer cell line poisons were discovered [23].

Knoevenagel condensations of 1H-indole-3-carbaldehyde with CH compounds yielded acrylamides and 3-(1H-indol-3-yl) acrylonitrile. Scientists made N-alkyl compounds by alkylating substances. Fatemeh Koohi et al. showed that leukaemia affects all ages and has distinct prevalence and incidence rates in Iran and overseas. It kills many, causes 8% of malignancies, and is expensive to treat. From 2003 to 2008, blood cancer incidence and locations were examined. Iran's Cancer Registry Center's 2003–2008 Health Deputy reports were used for this cross-sectional analysis. Join point Regression Program evaluated 18,353 reticuloendothelial and hematopoietic cancers' incidence and morphology [24]. Juliana G. Viana et al. employ gold nanoparticles in medicinal and chemical applications. Certain rules let bacteria create nanoparticles. This study synthesised

Frontier in Medical & Health Research
ISSN: (e) 3007-1607 (p) 3007-1593

metallic AuNPs from lavender blooms utilizing Priestia megaterium (CBMAI 2841). Culture broth reacted chloroauric acid. UV-Vis interaction creates bio-AuNPs after hours. TEM measured 45 nm bio-AuNPs after coalescence and self-assembly. Colloidal Bio-AuNPs liquid suspension was stable at 70 nm aerodynamic size and -18 mV zeta power. Bio-AuNPs catalysed malononitrile and aromatic aldehydes in Knoevenagel. The 30°C half-hour ethanol reaction yielded 0.4 mg AuNPs and Knoevenagel compounds [25].

Green science uses eco-friendly, efficient approaches, say Saeideh Tavakoli and Alireza Abbasi Solvothermal Co-Mg MOF synthesis using oxides. Multiple methods found them. The compound's putative basic and acidic sites catalysed the Knoevenagel condensation of malononitrile and benzaldehyde. Bimetallic MOF stimulant outperforms metal substitutions in catalysis. The cooperative effect causes the extracurricular effect when Mg^{2+} is introduced to Co MOF. After adjusting reaction conditions, malononitrile and various aldehydes produced quickly and in high yields at room temperature. The catalysts were stable and reusable after four reactions. The as-synthesized bimetal Co-Mg MOF performed well in Knoevenagel condensation with clean solvable ethanol [26].

2.2 Biological Activities

Aromatic aldehyde Knoevenagel compounds are potent antimicrobial. Their aromatic ring molecular structure may alter their potency against particular bacterial strains, whether they have electron-donating or electron-withdrawing groups. Just these chemicals are evaluated against Gram-positive and Gram-negative bacteria. Most antibacterial screenings detect Gram-negative and Gram-positive Escherichia coli and Staphylococcus aureus. Researchers also showed that nitro or halogen groups affect chemical effectiveness. Some research suggests aldehyde's electron-withdrawing groups let it pass via bacterial cell walls [27-35]. Laboratory tests measure inhibitory strength using agar well diffusion or micro dilution. Ampicillin and ciprofloxacin have millimeter-scale inhibitory zones. Most Knoevenagel compounds don't outperform antibiotics, but some do and require research. Several compounds hinder bacterial cell wall or DNA replication. Physically weakening bacterial defenses is possible with these drugs [28]. The antifungal properties are promising again. Test fungi include Candida Albicans, Aspergillums fumigates, and Cryptococcus neoformans. Fungal infections are tougher to treat than bacterial ones because they resemble human cells [29]. Fungal infections are tougher to treat than bacterial. Researchers find MIC values—chemical doses that no longer suppress fungal growth—using broth micro dilution or disc diffusion. Most Knoevenagel compounds have MICs like typical antifungals, even with synergistic medicines. Some compounds destroy fungus and bacteria, which is intriguing. Broad-spectrum antimicrobials may benefit from crossover activity [30].

3. RESEARCH METHODOLOGY

This research is done at the University of Sahiwal. Every chemical and reagent utilized in this investigation was analytical grade and came from reliable vendors such as Merck and Sigma Aldrich. Triethylamine (TEA) catalyst solutions, active methylene compounds, aromatic aldehydes, Other required reagents were used precisely as given, and solvents like ethanol as well as methanol were used in the quantities that were obtained and without further purification.

3.1 Apparatus

The Apparatus includes the round bottom flask, Hot plate, The magnetic stirrer and hot plate, Dropper, Reflux condenser, A thermometer, Separatory funnel, Beakers and graduated cylinders, Pipette with sucker, Weighing Balance, Spatula, TLC Plates, Capillary Tubes, Filter Paper, UV Lamp, TLC Chamber, Mobile Phase and China Dis

3.1.1 Chemicals and reagents

All the chemicals were taken from reputed sellers and not further purified. The chemicals used for synthesis of derivatives are salicylaldehyde, benzaldehyde Pyridine-4-Carbaldehyde, Diethyl Malonare, Malononitrile, Ethyl Acetoacetate, cyanoacetamide, sulphuric acid, pyridine and triethylamine. The Solvents used are methanol, ethanol, distilled water, DCM(Dichloromethane), n-hexane, acetone and chloroform.

Frontier in Medical & Health Research
ISSN: (e) 3007-1607 (p) 3007-1593

3.2 Instrumentation

In this section, we will study about instruments used for research.

3.2.1 LC, thin-layer chromatography

To monitor the reaction's progress via thin-layered chromatography, the researcher employed TLC plates. Pre coated silica gel 60 F_{254} plates were used. Tuned for effective separation of the starting components and product obtained were used ethyl acetate and hexane (3:1 blend). Visually, spots were seen under UV light at 253 nm and 364 nm. The percentages of the retention coefficients were obtained for both the product and starting ingredients to verify the completion of the reaction and progress of reaction. If the TLC has the clear spot in the product, the product is pure and more characterization methods can be done to explore the compounds in the product.

3.2.2 Infrared spectroscopy (IR)

Researchers describe synthesised molecules using infrared spectroscopy. IR detects organic molecule vibrations. And infrared absorption distinguishes wavelengths and functions. Fingerprint (1500-400 cm^{-1}) and functional group (4000-1500 cm^{-1}) infrared spectra exhibit distinct patterns. Functional groups like amine (-NH_2), carbonyl (C=O), and hydroxyl (-OH) are visible. Drug makers, organic chemists, and material scientists use IR spectroscopy to understand structures and purity. FTIR high-resolution spectra improve accuracy. The ATR analyses gas, liquid, and solid samples. Repetition without sample damage makes infrared spectroscopy promising. We use NMR and mass spectrometry because it cannot define molecular structures. Researchers describe synthesised molecules using infrared spectroscopy. IR detects organic molecule vibrations. And infrared absorption distinguishes wavelengths and functions. Fingerprint (1500-400 cm^{-1}) and functional group (4000-1500 cm^{-1}) infrared spectra exhibit distinct patterns. Functional groups like amine (-NH_2), carbonyl (C=O), and hydroxyl (-OH) are visible. Drug makers, organic chemists, and material scientists use IR spectroscopy to understand structures and purity. FTIR high-resolution spectra improve accuracy. The ATR analyses gas, liquid, and solid samples. Repetition without sample damage makes infrared spectroscopy promising. We use NMR and mass spectrometry because it cannot define molecular structures.

3.2.3 NMR spectroscopy:

Nuclear Magnetic Resonance (NMR) spectroscopy may verify chemical structure and purity. Typical of Knoevenagel products, NMR spectra of protons (^1H) and carbons (^13C) show critical functional groups such alkenes, carbonyls, and aromatic rings, therefore offering vital information on the molecular structure. Extended conjugation is a fundamental feature of these molecules; this is demonstrated by the downfield changes of the aromatic and vinylic protons. Additionally helping to determine connection and confirm the construction of the desired structures are integration values and coupling constants. Moreover, ^13C NMR spectra reveal the presence of significant carbonyl and alkene carbons, therefore distinguishing between distinct substitution patterns.

3.2.4 Hot Air Oven

Very essential in my MPhil research on synthesis of Knoevenagel derivative products is a lab hot air oven (brand: MEDFUTURE) which is used for drying the resultant products after synthesis and purification. During filtering and washing, a problem with the derivatives is that residual solvents or moisture may be retained which interferes with further characterization and biological assessment. If arrangements of the pure chemicals in a clean petri dish or watch glass, and drying at a regulated temperature (40–60°C) for many hours will ensure total solvent evaporation no breakdown, then the oven is guaranteed to do so. With this procedure, the purity, stability and yield of the derivatives are improved such that they are suitable for various analytical methods.

3.2.5 Rotary Evaporator

Researchers dried with Yamato's rotary evaporator. Low-pressure organic synthesis and purification require the rotary evaporator (Rotovap). This device lets chemists remove solvents from a solution without heating the delicate material. Academics and industry use the Rotovap system because it meets lab needs. For laboratory medicinal research, the device concentrates; solvent filters, and recycles

Frontier in Medical & Health Research
ISSN: (e) 3007-1607 (p) 3007-1593

chemical reaction mixtures without thermally damaging sensitive molecules. The condenser, vacuum pump-connected spinning flask, and heated water bath slowly evaporate low-boiling liquids. Heat degradation protector Rotovap purifies process intermediates, extracts concentration, and isolates pure compounds. Biological testing and Knoevenagel derivative synthesis, purification, and characterization require solvent removal.

3.3 General Procedure for Synthesis of Knoevenagel derivatives

Knoevenagel condensation of an aromatic aldehyde (0.002mmol) with an active methylene molecule in an environment of a basic catalyst like triethylamine produced the derivatives. In a round-bottom flask, aromatic aldehyde was dissolved in ethanol and active methylene compound was placed while stirring. A catalytic concentration of triethylamine/pyridine started the process. The reactants determined whether the mixture was refluxed or stirred at room temperature. TLC with a 1:4 mixture of ethyl acetate and hexane was used to monitor the reaction after letting it rest and mix at room temperature. For one night, this reaction flask was left alone. Crushed ice was added after the reaction and stirred until solidified. Following filtering and washing with cold water to remove debris, the yellow solid was cleaned with ethanol and allowed to settle to form clean crystals. Before spectroscopy, I physically inspected the goods. The final result was determined by IR, NMR, and mass spectrometry.

3.3.1 Molecular Docking Studies

We used AutoDock Vina for docking; setting grid boxes around the active site residues of the proteins involved. Additional inspection of postures was required because docking provided binding affinity (in kcal/mol). The docked complexes were examined in three dimensions using PyMOL and the interactions discovered in two dimensions, including hydrophobic, π–π and hydrogen bond contacts, by relying on Discovery Studio Visualizer and LigPlot+ following docking. Analyzing how the synthetic compounds interact with leukemia targets suggested they might be effective against blood cancer diseases.

3.3.2 3-Acetyl-2H-chromen-2-one (1a)

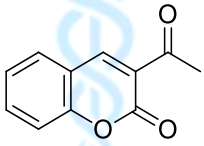

Yield: 92%
Melting Point: 119–121°C
Color: Yellow
Physical Appearance: Needle shape yellow crystals
FT-IR (K Br, cm⁻¹): (3402 cm^{-1} C-H), (1739 cm^{-1} C=O), (1604 cm^{-1} C=O), (1604 cm^{-1} C=C), (1352 cm^{-1} C-O).
1 H-NMR: 1 H-NMR (500 MHz, DMSO- d6, δ=part per million [ppm]); 2.59: (s, 3H, CH3), 8.63: (s, 1H, Ar-H), (7.39-7.94)m, 4H,)

3.3.3 (1E, 4E)-1, 5-di (3815yridine-4-yl)penta-1,4-dien-3-one (2a)

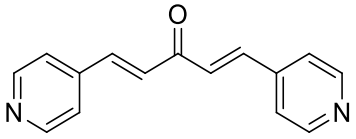

Yield: 90%
Melting Point: 130-135°C
Color: Light yellow
FT-IR (KBr cm-1): (3400cm^{-1} CH),(1725cm-1(1600cm^{-1}C=O),(1600cm^{-1}C=C),(1350cm^{-1} C-N)
1 H-NMR: 1 H-NMR (500 MHz, DMSO- d6, δ=part per million [ppm]); 7.25(d, 4.5 Hz, 2H); 8.45(d, 4.5Hz, 2H); 5.55(d, 2Hz, 1H); 4.55(d, 2Hz, 1H)

Frontier in Medical & Health Research
ISSN: (e) 3007-1607 (p) 3007-1593

3.3.4 (2E, NE)-2-cyano-N-(2-hydroxybenzylidene)-3-(2-hydroxyphenyl) acrylamide (3a)

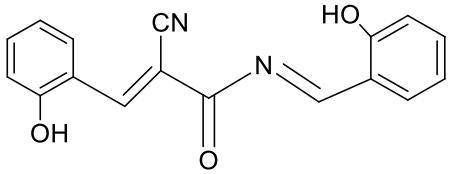

Yield: 91%
Melting Point: 210-215°C
Color: Yellow orange
Physical Appearance: Yellow orange solid
FT-IR (K Br, cm⁻¹): (3430 cm^{-1} C-H), (3430 cm^{-1} C-H), (3200 cm^{-1} -OH), (2250 cm-1 -CN), (1610 cm^{-1} C=O), (1610 cm^{-1} C=C), (1350 cm^{-1} C-O),
1 H-NMR: 1 H-NMR (500 MHz, DMSO- d6, δ=part per million [ppm]); 9.55(s, 4Hz 1H),8.9(s,1.5Hz,1H),8.4(s,6.5Hz,1H),8.45(s,6.5Hz,1H),8.0(d,1Hz,2H),7.75(d,1.5Hz,2H),7.55(t,1.5Hz,2H),7.4(t,1.5Hz,2H),7.25(t,7.5Hz,2Hz),7.2(d,12Hz,2H),7.0(d,7.5Hz,2H),6.95(t,6,95Hz,2Hz).

3.3.5 €-2-cyano-3-(3816yridine-4-yl) acrylamide (4a)

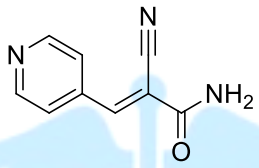

Yield: 90%
Melting Point: 205-210°C
Color: Off white to pale yellow
Physical Appearance: Crystalline solid
FT-IR (K Br, cm⁻¹): (3402 cm^{-1} N-H), (2250 cm^{-1} -CN), (1600 cm^{-1} C=O), (1600 cm^{-1} C=C), (1350 cm^{-1} C-N).
1 H-NMR: 1 H-NMR (500 MHz, DMSO- d6, δ=part per million [ppm]); 8.18(s, 3Hz 1H), 7.95(d, 6.5Hz, 2H), 7.77(s, 6.5Hz, 2H), 7.57(d, 5Hz, 2H).

3.3.6 €-Ethyl 3-(3816yridine-4-yl) acrylate (5a)

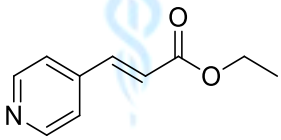

Yield: 90%
Melting Point: 56-58°C
Color: Pale Yellow
Physical Appearance: Crystalline powder
FT-IR (K Br, cm⁻¹): (3403 cm^{-1} C-H), (2250 cm-1 -CN), (1601 cm^{-1} C=O), (1601 cm^{-1} C=C), (1349 cm^{-1} C-O),
1 H-NMR: 1 H-NMR (500 MHz, DMSO- d6, δ=part per million [ppm]); 8.8(s, 1.5Hz 2H),8.5(s,3Hz,1H),7.8(d,1.5Hz,2H),7.25(s,2Hz,1H),3.5(q,7.1Hz,2H),1.0(t,7Hz,3H).

3.3.7 Diethyl 2-benzylidenemalonate (6a)

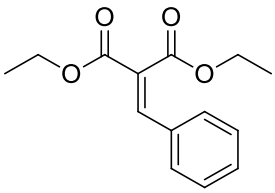

Yield: 92%
Melting Point: 75-78°C
Color: Pale yellow to yellow crystalline solid

Frontier in Medical & Health Research
ISSN: (e) 3007-1607 (p) 3007-1593

Physical Appearance: Crystalline solid
FT-IR (K Br, cm^{-1}): (3406 cm^{-1} C-H), (1763 cm^{-1} C=O), (1607 cm^{-1} C=C), (1208 cm^{-1} C-O),
1 H-NMR: 1 H-NMR (500 MHz, DMSO- d6, δ=part per million [ppm]); 8.7(s, 1.5Hz,1H),7.95(d,6.5Hz,2H),7.75(t,6.5Hz,1H),7.45(t,6.5Hz,2H),4.3(q,5Hz,4H),1.3(t,7Hz,6H).

4. RESULTS AND DISCUSSION

The approach shown in the scheme below was used to derivativized the target chemicals. The olefinic α-β unsaturated compounds were synthesised with high yield and purity using the Knoevenagel condensation. The different modified compounds were prepared using cyanoacetamide, ethyl acetoacetate, diethyl malonate, and malononitrile. Using molecular docking and biological activities, the potential of these synthesized molecules was assessed.The synthesis of the Knoevenagel derivatives **(1a-6a)** included combining active methylene compounds with various aromatic aldehydes in ethanol while stirring for one to three hours while triethylamine was present. After cooling to room temperature, the liquid was poured into cold water to cause precipitation. After filtering, the pure chemicals were gathered.

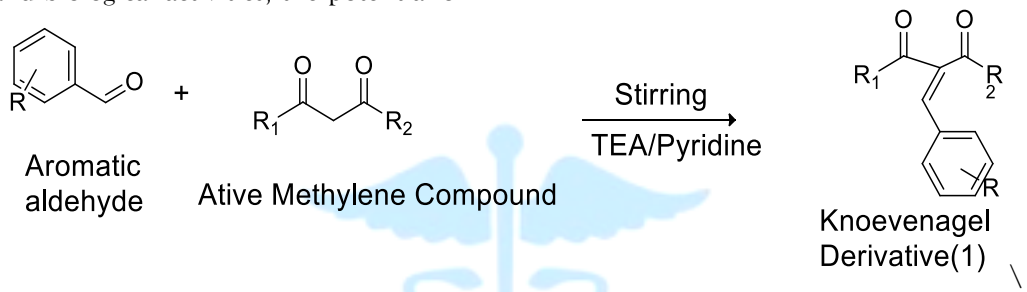

R=R_1=R_2=OCH_3, OC_2H_5, CN etc.

Figure 4.1: Scheme for the Synthesis of knoevenagel compounds

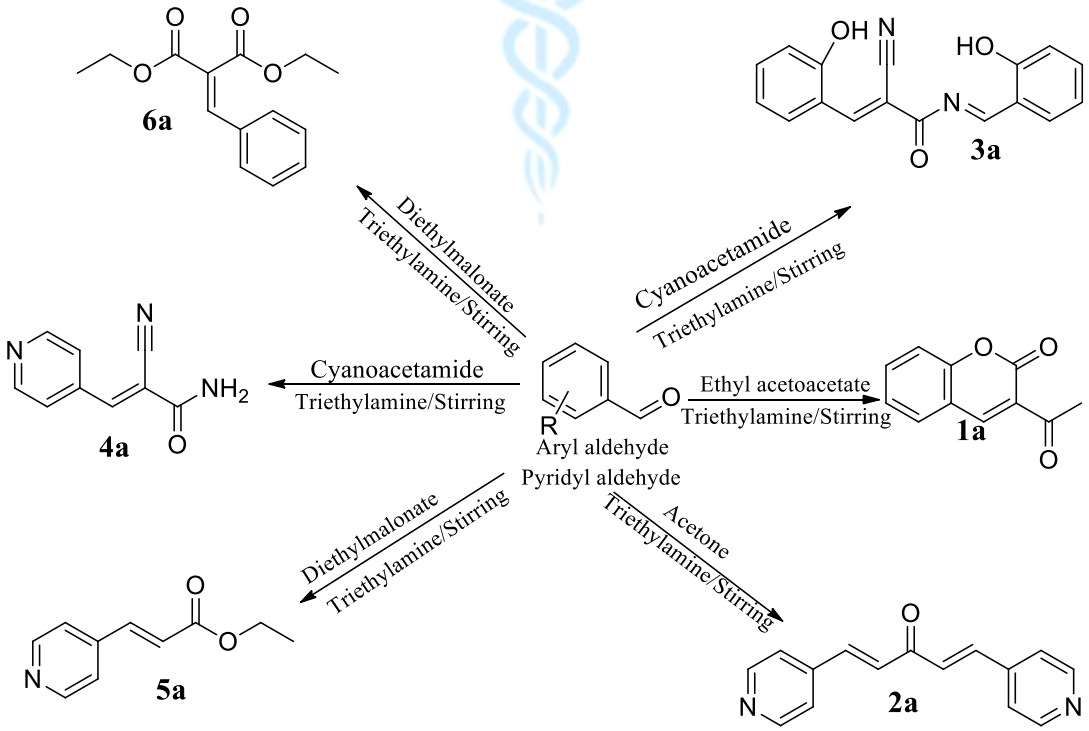

Figure 4.2: Scheme for the Synthesis of knoevenagel compounds (1a-6a)

Frontier in Medical & Health Research

ISSN: (e) 3007-1607 (p) 3007-1593

Before spectroscopy, I physically inspected the goods. All of the produced compounds were examined using IR and 1H-NMR spectroscopy. Scheme 1 depicts the general structure, which is verified by spectral methods. The FTIR shows an NH absorbed peak somewhere between 3700–3800 cm-1 and C=O at about 1600–1700 cm-1. In a comparable manner proton NMR verified NH at 8–9 ppm. The synthesis of 3-Acetyl-2H-chromen-2-one used Knoevenagel condensation. Ten mL ethanol, 0.002 mmol salicylaldehyde, and ethyl acetoacetate were mixed in a clean round-bottom flask. Two to three triethylamine drops helped condensation A 1:4 mixture of ethyl acetate and n-hexane was used to develop the reaction solution for 4–5 hours at room temperature. TLC tracked progress. It stayed overnight. Ice water cooled reaction. Water filtration and cold water washing crystallised yellow ethanol from crude solid. Product inspection preceded spectroscopy. The UV-Vis absorption of 3-acetyl-2H-chromen-2-one reveals a conjugated structure with a strong λ-max 330 nm band. The band displays π→π* transitions in the conjugated chromenone system. Structure confirmed by infrared. 3402 cm-1 showed aromatic C-H stretching. The carbonyl (C=O) group of the chromenone core showed a significant vibrational band at 1739 cm^{-1}. A second band at 1660 cm^{-1} indicated the ketonic carbonyl (acetyl group) presence. Aromatic C=C vibrations were found at 1604 cm^{-1}, while C–H in-plane vibrations were observed between 900 and 750 cm^{-1}. C-O is 1352 cm-1. A mass spectrum peak at m/z 188.18 [M^+] confirmed the chemical formula of 3-acetyl-2H-chromen-2-one ($C_{11}H_8O_3$). The structure is supported by UV, IR, and MS spectra

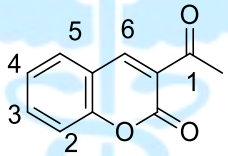

Figure 4.3: Proton-labelled structure of compound 1a

3-acetyl-2H-chromen-2-one (1) was subjected to a 1H NMR study in DMSO-d_6 using a spectrometer set to 500 MHz. The methyl group in the acetyl group was represented by a singlet with amplitude three at δ 2.6 ppm. A singlet at δ 8.6 ppm was produced by an olefinic proton at position 6 (H-6) of the chromenone ring system. The aromatic area was most clearly seen between δ 7.4 and 8.0 ppm. Doublets with the same coupling constant were observed at positions H-5 and H-2 in both δ 7.4 and δ 7.9 ppm, confirming their presence in the benzene ring. As a result, they were allocated to H-5 and H-2, respectively, both of which were undergoing ortho coupling. The proton located at the H-3 position in the molecule's aromatic ring is represented by a doublet of doublets at δ 7.7 ppm. The proton is positioned as H-4 and has a doublet of doublet at δ 7.5 ppm. The synthetic compound's structure of 3-acetyl-2H-chromen-2-one is confirmed by the experimental spectra and chemical shifts [31].

Table 4.1: ^{1}H-NMR (500 MHz) Spectral Data of 1a in DMSO

Position	^{1}H, δ_H multiplicity, (J in Hz)
1	2.6, s (3H, 0Hz)
2	7.9, d (1H, 1Hz)
3	7.7, t (1H, 6.5Hz)
4	7.5, t (1H, 6.5Hz)
5	7.4, d (1H, 1Hz)
6	8.6, s (1H, 1.5Hz)

The molecule under investigation is (1E, 4E)-1, 5-di(pyridin-3-yl)penta-1,4-dien-3-one according to mass, UV, and IR spectra. We discovered ethanol's conjugated dienone system causes a π→

Frontier in Medical & Health Research
ISSN: (e) 3007-1607 (p) 3007-1593

π* transition at 318 nm using UV-Vis spectroscopy. Primary absorption band at 1600 cm^{-1} in infrared spectra indicates conjugated carbonyl (C=O) group stretching vibration. The pyridine group's stretching of C=C and C=N causes bands at 1600 cm^{-1}, while C-N is visible at 1350 cm-1. A peak [M^+] at m/z 236 matched the chemical formula $C_{15}H_{12}N_2O$, revealing the molecule's molecular weight in the mass spectrum. The pyridine group is common in M/z 121. Our spectrum confirms the simple production and robust structure of (1E, 4E)-1,5-di(pyridin-3-yl)penta-1,4-dien-3-one.

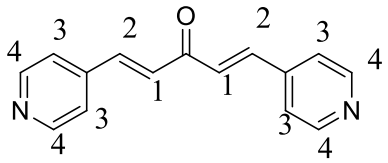

Figure 4.4: Proton-labelled structure of compound **2a**

(1E, 4E)-1,5-di(pyridin-3-yl)penta-1,4-dien-3-one (2)'s ^1H NMR spectra was recorded using 500 MHz in DMSO. The spectrum showed the expected signals because of the pyridine groups and the connected enone system. The olefinic protons, which show the trans (E) arrangement across both double bonds as H-2 and H-1, were observed as two separate doublets at 5.55 ppm (2H) and 4.55 ppm (2H), both with a coupling constant of J = 2 Hz. The pyridine rings were the source of signals in the aromatic area. The H-3 and H-4 protons exhibit doublets at 7.25 ppm (J = 4.5, 2H) and 8.45 ppm (J = 4.5, 2H), respectively. The behavior of these aromatic protons and their coupling constants indicated that the compound has a balanced structure, playfully implying that the pyridine ring is in the third position. The spectral data validated the title's assumption about the configuration of (1E, 4E).The experimental data and chemical shift measurements show that the molecule made matches (1E, 4E)-1, 5-di (pyridin-3-yl) penta-1, 4-dien-3-one as shown in figure.

Table 4.2: ^1H-NMR (500 MHz) Spectral Data of 2a in DMSO

Position	^1H, δ_H multiplicity, (J in Hz)
1	4.55, d (2H, 2Hz)
2	5.55, d (2H, 2Hz)
3	7.25, d (2H, 4.5Hz)
4	8.45, d (2H, 4.5Hz)

Studies using FT-IR and HNMR spectrometry determined the structure of (2E,NE)-2-cyano-N-(2-hydroxybenzylidene)-3-(2-hydroxyphenyl) acrylamide. The infrared spectrum revealed a distinct absorption band at 2250 cm^{-1}, indicating the cyano (–C≡N) stretching vibration. Amide's C=O stretching vibration was observed at 1605 cm^{-1}, while phenolic groups formed a broad O–H stretching band peaking at 3302 cm^{-1}. A band at 1690 cm resurfaced the Schiff base moiety's C=N stretching vibration. Spectroscopic characteristics show that the molecule was produced and is structurally intact.

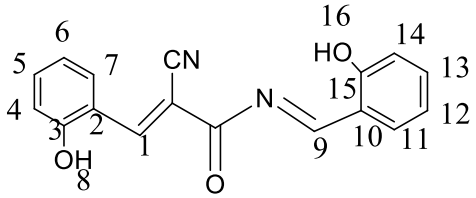

Figure 4.5: Proton-labelled structure of compound 3a

Frontier in Medical & Health Research
ISSN: (e) 3007-1607 (p) 3007-1593

The structure of (2E, NE)-2-cyano-N-(2-hydroxybenzylidene)-3-(2-hydroxyphenyl) acrylamide can be verified using 500 MHz ^{1}H NMR in DMSO-d_6. Combining the spectra revealed the target chemical. Nearby hydrogen bonds caused a strong singlet at δ ppm, indicating the phenolic -OH group is downfield. The amide-NH proton is affected by hydrogen bonds and DMSO solvation, resulting in a broad signal at δ 9.6 ppm at position H-9 in the spectrum. 2-hydroxyphenyl and salicylaldehyde ring protons were visible as peaks with chemical shifts from 6.9 to 8.0 ppm in the aromatic area. The signal at 9.55 ppm is correct for the imine proton (-CH=N-) since there are no neighbouring protons to induce coupling. A cluster of doublets and multiplets at δ 7.60-6.90 ppm confirmed protons in both aromatic regions, aligning with other data. They provided multiplicity and coupling patterns that matched substitution patterns. All tests' chemical shifts and coupling patterns allowed acrylamide derivative synthesis. Also, the olefinic proton near the cyano group appeared as a singlet at H-1 at δ8.9 ppm in the spectrum. Singlets of -OH protons at H-8 and H-16 are found at 8.4 and 8.45 ppm. The aromatic ring has four triplets at positions H-13, H-12, H-5, and H-6 in the HNMR spectra at 7.55, 7.4, 7.25, and 7.95 ppm. Four doublets with chemical shift values of 8.0 ppm, 7.75 ppm, 7.2 ppm, and 7.0 ppm at positions H-1, H-14, H-4, and H-7 indicate two aromatic rings in the molecule. Figure shows that the produced molecule is (2E, NE)-2-cyano-N-(2-hydroxybenzylidene)-3-(2-hydroxyphenyl)acrylamide based on chemical shift measurements and experimental data.

Table 4.3: ^{1}H-NMR (500 MHz) Spectral Data of 3a in DMSO

Position	^{1}H, δ_H multiplicity, (J in Hz)
1	4.55, d (2H, 2Hz)
2	5.55, d (2H, 2Hz)
3	7.25, d (2H, 4.5Hz)
4	8.45, d (2H, 4.5Hz)

Spectrum features confirm (E)-2-cyano-3-(pyridin-4-yl) acrylamide's unique structure. The infrared spectrum shows a band at 2250 cm^{-1}, indicating nitrile (C≡N) stretching vibration. N-H vibrations are found in a medium band below 3402 cm^{-1}, while the amide group's carbonyl (C=O) has a strong band near 1600 cm^{-1}. IR spectrum bands at 1600 cm^{-1} suggest aromatic and vinyl C=C functions. Removing the amide or nitrile groups creates fragmentation peaks, confirming the peak pattern.

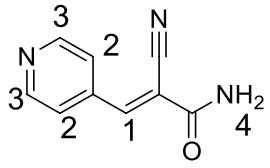

Figure 4.6: Proton-labelled structure of compound 4a

The proton-containing parts of (E)-2-cyano-3-(pyridin-4-yl)acrylamide can be identified in DMSO-d_6 using a 500 MHz ^{1}H NMR spectrum. The amide -NH proton exhibits a singlet at δ 7.77 ppm. Hydrogen bonding and the carbonyl group shielding the hydrogen atom make this signal a high-field spectrum. Spectrum shows aromatic region with two symmetrical doublets at 7.57 and 7.95 ppm at H-2 and H-3. The first peak at δ 7.57 ppm (J=6Hz) is integrated for two protons. The less field-protected ortho positions next to the nitrogen atom give the pyridine ring protons. The peak at δ 7.95 ppm (J=6Hz) is a doublet caused by two protons. Additionally, a vinylic proton (=CH) appears as a singlet at δ 8.18 ppm with J = 5 Hz coupling constant, indicating an E-configuration double bond (Trans). Overall, the proton NMR spectrum confirms the compound's composition, showing an E-configured α, β-unsaturated system with pyridine and nitrile groups.

Frontier in Medical & Health Research
ISSN: (e) 3007-1607 (p) 3007-1593

Table 4.4: ^{1}H-NMR (500 MHz) Spectral Data of 4a in DMSO

Position	^{1}H, δ_H multiplicity,(J in Hz)
1	8.18, s (1H, 5Hz)
2	7.57, d (2H, 6Hz)
3	7.95, d (2H, (6Hz)
4	7.77, s (2H, 0Hz)

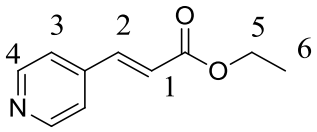

Figure 4.7: Proton-labelled structure of compound 5a

KBr pellets were IR-tested for (E)-ethyl 3-(pyridin-4-yl) acrylate. Molecular group absorption bands are fingerprint-like. The compound contains acrylate ester, indicated by a strong absorption peak at 1601 cm^{-1} from the ester carbonyl (C=O). The C=C vibration at 1601 cm^{-1} between the double bond and ring confirms conjugation. The pyridine ring's C=N and C=C bonds stretch at 1601 cm^{-1}, causing the frequency. Aromatic and vinylic protons stretch at 2900-3500 cm^{-1}, while aliphatic ethyl C–H stretches at 2850-2960 cm^{-1}. C–O vibrations in organic compounds cause a peak at 1349 cm^{-1} for the ester group, while out-of-plane C–H bond bending in aromatic rings causes vibrations at 7500-860 cm^{-1}. The ester, pyridine, and acrylic system exist. Compound (E)-ethyl 3-(pyridin-4-yl)acrylate was characterised using 500 MHz ^{1}H NMR in DMSO-d_6, which matched molecule expectations. The ester terminal methyl at H-6 was found to be a triplet at δ 1.1 ppm (J = 7.1 Hz, 3H). The quartet at δ 3.5 ppm (J = 7 Hz, 2H) represents the methylene group next to ester oxygen at position H-5. Proton near carbonyl group exhibited doublet at δ 7.5 ppm (coupling constant: 2 Hz), while vinylic proton near pyridine ring exhibited doublet at δ 8.45 ppm (coupling constant: 3 Hz) at positions H-1 and H-2.Their coupling constant confirms trans double bond. The aromatic region of the pyridine molecule exhibited two doublets at δ 8.8 ppm (J = 1.5 Hz, 2H) and δ 7.8 ppm (J = 1.5 Hz, 2H) at positions H-4 and H-3, the ring carbon protons Matching chemical shifts and patterns in the spectrum confirmed [E-ethyl 3-(pyridin-4-yl)-acrylate] preparation.

Table 4.5: ^{1}H-NMR (500 MHz) Spectral Data of **5a** in DMSO

Position	^{1}H, δ_H multiplicity,(J in Hz)
1	7.5, d (1H, 2Hz)
2	8.45, d (1H, 3Hz)
3	7.8, d (2H, 1.5Hz)
4	8.8, d (2H, 1.5Hz)
5	3.5,q (2H, 7Hz)
6	1.1, t (3H, 7.1Hz)

Main peaks in Diethyl-2-benzylidenemalonate's KBr pellet FT-IR spectrum indicate key groups. The presence of a prominent ester carbonyl (C=O) band at 1763 cm^{-1} suggests two ester groups in the molecule. A 1601 cm^{-1} band indicates the exocyclic phenyl ring's C=C bond vibration, while multiple C=C peaks in the 1450-1650 cm^{-1} range suggest a monosubstituted benzene ring. Spectra reveal protons' aromatic C-H vibrations at 3406 cm^{-1}, ethyl ester C-H stretches from 2850 to 2970 cm^{-1}, and esters' C-O stretching at 1208 cm. C–H bond vibrations in aromatic rings stretch and bend out of the plane (740-770 cm^{-1}). These IR absorptions confirm diethyl benzylidenemalonate's ester-aromatic structure.

Volume 4, Issue 3, 2026

Frontier in Medical & Health Research

ISSN: (e) 3007-1607 (p) 3007-1593

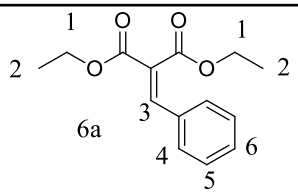

Figure 4.8: Proton-labelled structure of compound 6a

The structure of Diethyl-2-benzylidenemalonate was determined using 500 MHz ^{1}H NMR spectroscopy in DMSO-d_6. The spectrum resonances match the model. A singlet at δ 8.7 ppm indicates the vinylic proton (–CH=) of the benzylidene moiety, located next to the aromatic ring and ester groups at position H-3. Several multiplets near δ 7.30-8.45 ppm, representing five protons of a single benzene group, confirmed a monosubstituted phenyl ring. Two ethyl ester groups had distinct signals: methylene group protons (–CH_2–) appeared in quartets at δ 4.3 ppm (J = 5 Hz, 4H), while methyl group protons (–CH_3) appeared as triplets at δ 1.3 ppm (J = 7.1 Hz, 6H).Two protons form a doublet at 7.9 ppm at H-4.At positions H-5 and H-6, a triplet of 2 protons appeared at 7.45 ppm and a triplet of 1 at 7.75 ppm. The molecule behaved like two identical ethyl ester groups. Using fourier-transformed NMR data, Diethyl-2-benzylidenemalonate was confirmed as a pure substance.

Table 4.6: ^{1}H-NMR (500 MHz) Spectral Data of 6a in DMSO

Position	^{1}H, δ_H multiplicity,(J in Hz)
1	7.5, d (1H, 2Hz)
2	8.45, d (1H, 3Hz)
3	7.8, d (2H, 1.5)
4	8.8, d (2H, 1.5)
5	3.5, q (2H, 7Hz)
6	1.1, t (3H, 7.1Hz)

Table 4.7: FT-IR spectral data of the synthesized compounds (1a–6a)

Compounds	FT-IR absorption bands , νmax (cm^{-1}) and assignment of functional groups
1a	3402 (C–H), 1739 (C=O), 1604 (C=C), 1352 (C–O)
2a	3400 (C–H), 1725 (C=O), 1600 (C=C,C=N,C=O), 1350 (C–N)
3a	3400 (C–H), 3302 (O–H, N–H), 2255 (C≡N), 1605 (C=O/C=C), 1232 (C–O)
4a	3402 (N–H), 2250 (C≡N), 1600 (C=O/C=C), 1350 (C–N)
5a	3403 (C–H), 1601 (C=O/C=C), 1349 (C–O)
6a	3406 (C–H), 1763 (C=O), 1601 (C=C), 1208 (C–O)

4.1 Biological Activities

In this section, we will explain the biological activities of the synthesized compounds. It includes the procedure and their potential etc.

4.1.1 Antibacterial Activity

The Knoevenagel condensation method efficiently synthesizes α,β-unsaturated carbonyl molecules with high biological activity in medicinal chemistry. Knoevenagel derivatives showed promising Gram-positive and Gram-negative antibacterial activity in several studies. Ethyl cyanoacetate and its active methylene compound and aromatic aldehyde derivatives inhibit S. typhi, E. coli, and S. aureus [32-40].Thru chemical and structural flexibility, these substances can be modified to increase bioactivity by adding metal ions, hydroxyl functionality, or electronic withdrawing groups. Coumarin derivative-based Knoevenagel has lower MIC values than several well-known antibiotics. Activity rises when metal complexation with Knoevenagel ligands improves membrane stability and permeability. Our drug development time results suggest Knoevenagel derivatives

Frontier in Medical & Health Research
ISSN: (e) 3007-1607 (p) 3007-1593

could scaffold new anticolleric drugs due to antibiotic resistance [41-50].

The disc diffusion test was used to evaluate the synthetic derivatives' antibacterial activity against Gram-positive Bacillus subtilis, Staphylococcus aureus, E. coli, and P. aeruginosa. The study compared compounds using inhibition zone analysis to 100 µg/mL conventional ampicillin. Each strain tested showed significant antibacterial effects from compound 3's aromatic ring structure's para-nitro group. Research shows that nitrous electron-withdrawing group improves chemical interactions with bacterial membranes by allowing lipid contact. Hydroxyl modification increased compound 5's S. aureus-fighting efficacy due to hydrogen bonding [51-60].

Because electron-donating groups on the double bond reduced electrophilic and biological tolerance, compounds 2 and 6 had low bacterial activity. Compound 7's size prevented it from penetrating cell membranes, limiting its voltage-holding antibacterial properties. Nitro and halogen compounds with electron-withdrawing groups kill bacteria better than those with longer or bulkier groups. Deliberate functional group modification improves antibacterial efficacy. The Knoevenagel core can be coupled with functional groups to create novel antibacterial drugs. Future research should use molecular docking and MIC testing to improve these compounds' activity. Compound 4 was most antibacterial. Furthermore, Derivative 3 showed promising antibacterial activity. [61-69].

Table 4.8: Antibacterial activity of knoevenagel derivatives

Compounds	Antibacterial Activity: Zone of Inhibitions against Staphylococcus Aureus (mm)	Activity Level
1a	19.82 mm	Strong
2a	24.67 mm	Strong
3a	30.04 mm	Strong
4a	21.49 mm	Strong
5a	25.25 mm	Strong
6a	21.68 mm	Strong

4.1.2 Antifungal Activities

This section describes the antifungal properties of synthetic Knoevenagel derivatives made from substituted aromatic aldehydes. Researchers evaluated antifungal efficacy using Mueller Hinton Agar (MHA) well diffusion, which measured zone of inhibition (ZOI) diameters to determine fungal growth inhibition. Isolated fungal colonies were added to sterile saline to make the suspension. Using a quartz cuvette with a path length of 1.0 cm and a Shimadzu UV-Vis 650 PC spectrophotometer set at 420 nm, the turbidity was measured. OD measurements determined fungal cell concentration. Following suspension standardization, researchers used 10-fold serial dilution to achieve the desired cellular density for the bioassay protocol after solidification [70-78]. To the diluted fungal slurry on agar plates, four drops of 100 µL volume were added. Using sterile cotton swabs, the inoculum was spread evenly across the fungal growth region. With sterile 1 mL micropipette tips, uniform wells were made in agar. Triethylamine-catalyzed reactions between malononitrile and aromatic aldehydes produced Knoevenagel derivatives, which required removing extra agar plugs for sterility. Purified raw chemicals were dissolved in 1 milliliter of distilled water to dilute test solutions. The researcher used a sterile pipetting procedure to add 200 µL of each solution into the wells. Plates were incubated at 37°C for a day. Using forceps to prevent contamination, the assay used pure water as the negative control and fluconazole as the positive control. Following incubation, clear inhibition zones appeared around a few of the wells. Researchers used a caliper that provided readings in millimeters or a transparent ruler to measure the widths of the zones under investigation. By comparing the compounds' measured zone of inhibition size to the standard control size,

Frontier in Medical & Health Research
ISSN: (e) 3007-1607 (p) 3007-1593

researchers were able to classify their activities as strong, moderate, mild, and inactive [79-85].

Table 4.9: Antifungal activity of aromatic aldehydes derivatives

Compounds	Antifungal Activity: Zone of Inhibitions against Candida Albicans (mm)	Activity level
1a	21.28 mm	Strong
2a	11.53 mm	Mild
3a	16.63 mm	Moderate
4a	17.31 mm	Moderate
5a	18.64 mm	Strong
6a	23.48 mm	Strong

New antifungal properties found during synthesis varied depending on aromatic aldehyde and active methylene structures. The strongest antifungal effects were found in pyridine-4-carbaldehyde derivatives compared to benzaldehyde and salicylaldehyde. Pyridine folk's electron-enriching ring nitrogen makes it more polar and electron-binding, which may damage fungal enzymes and cell surfaces. Because salicylaldehyde hydroxyl group may participate in hydrogen bonding interactions that enhance biological activity, derivatives made from it may have greater activity than those made from unsubstituted benzaldehyde [86-92]. Of all aldehyde classes, malononitrile derivatives were most effective against fungus among active methylene compounds. Two strong electron-withdrawing cyano groups boost the molecule's membrane-penetration and electrophilicity. Diethyl malonate and ethyl acetoacetate had limited target interaction with fungal agents, limiting their derivative compounds' antifungal activities to mild to moderate. Diethyl malonate and ethyl acetoacetate derivatives had low to moderate antifungal effects, but their lack of polar structures and acid functionality prevented them from targeting fungal targets [93-98]. The substance has a significant capacity to function as a primary antifungal treatment; hetero aromatic aldehydes and electron-withdrawing active methylene components enhance antifungal efficacy; altering the functional group structure improves antifungal action; and the malononitrile derived from pyridine-4-carbalde has antifungal properties [99,100].

4.2 Molecular Docking Studies for Blood Cancer

In this section, we will discuss about molecular docking studies for blood cancer potential of synthesized knoevenagel compounds.

Table 4.10: Evaluation of antiblood cancer potential

Compounds	Protein/Enzyme
1a-6a	Extracellular superoxide dismutase (SOD3), a key antioxidant enzyme, demonstrates potential anti-blood cancer activity by mitigating oxidative stress in hematological malignancies. The human SOD3 structure (PDB ID: 4M0Z) provides critical insights into its molecular function and therapeutic targeting.

4.2.1 Computational Evaluation of Knoevenagel Derivatives as Potential SOD3 Inhibitors

Six knoevenagel-derived compounds (1a-6a) were computationally investigated as potential inhibitors of extracellular superoxide dismutase (SOD3, PDB ID: 4M0Z), a blood cancer therapeutic target. To determine structure-activity relationships and binding mechanisms, AutoDock Vina was used for rigorous molecular docking. Conformational sampling and charge assignment were used to prepare ligands, while structural optimization and active site characterization were done to An exhaustiveness parameter of 16 was used for docking simulations to explore binding conformations. With a docking score of -4.953 kcal/mol ,

Frontier in Medical & Health Research
ISSN: (e) 3007-1607 (p) 3007-1593

compound 2a was the most potent candidate after analyzing binding affinities. Affinity hierarchy (2a > 3a > 4a > 6a > 1a > 5a) shows significant structure-activity trends in this chemical series. Without polar contacts, Compound 1a bound moderately (-3.927 kcal/mol) to ALA389, LEU489, and ILE369 via exclusive hydrophobic interactions, suggesting blood-brain barrier penetrance. Superior performance of compound 2a is due to its diverse interaction network, including two hydrogen bonds with catalytic residues ASP500 and ASN487, one carbon-hydrogen bond, and extensive π-alkyl interactions with LEU489 and ILE369. These polar-hydrophilic contacts may inhibit competitively.

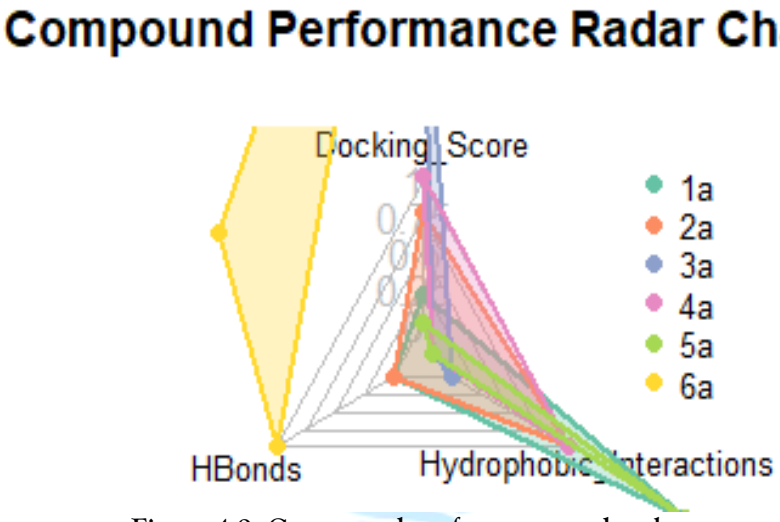

Figure 4.9: Compound performance radar chart

Compound **3a** (-4.754 kcal/mol) exhibited specific binding patterns, including hydrogen bonding with CYS442, π-π T-shaped stacking with PHE437 near the catalytic center, and hydrophobic interactions with VAL377 and MET438, suggesting potential allotter Compound **4a** (-4.157 kcal/mol) balanced interactions with polar (GLU436) and hydrophobic (ILE369, ALA389) residues, while compound **6a** (-3.887) uniquely engaged basic residues LYS391 and ARG486 and catalytic CYS442, promising novel inhibition mechanisms The unexpectedly weak binding of compound **5a** (-1.975 kcal/mol) despite four hydrogen bonds emphasizes spatial orientation and steric compatibility in inhibitor design.
A structure-activity relationship analysis showed several binding efficacy trends. Top-performing compounds **2a** and **3a** formed multiple polar contacts with catalytic residues ASP500, ASN487, and CYS442, indicating hydrogen bonding capacity determined affinity. Hydrophobic complementarity was essential, as evidenced by consistent π-alkyl interactions with ALA389, LEU489, and ILE369 in active compounds. Compound **3a**'s favorable aromatic stacking interaction suggests future analogues should retain or add aromatic moieties. Compound **5a**'s poor performance despite hydrogen bonding potential showed that steric factors significantly affected binding. Direct active site competition by catalytic residues (ASP500, ASN487), allosteric modulation by structural elements (PHE437, CYS442), and redox interference by cysteine coordination are possible inhibition mechanisms. Computational predictions from static docking models without solvation effects or entropic contributions should be interpreted with caution. Focus on enzymatic inhibition and cellular studies in blood cancer models, then optimize structure for hydrogen bonding with ASP500/ASN487, hydrophobic packing in ALA389/LEU489 pocket, and aromatic group introduction for π-π stacking interactions. Due to its optimal hydrogen bonding and hydrophobic interactions, compound **2a** is the best SOD3 inhibitor in this systematic docking study. The study emphasizes targeting catalytic residues (ASP500, ASN487) and the hydrophobic subpocket (ALA389, LEU489, ILE369)

Frontier in Medical & Health Research
ISSN: (e) 3007-1607 (p) 3007-1593

simultaneously in medicinal chemistry. These findings suggest developing novel knoevenagel-based hematological malignancy treatments, with compound **2a** as a promising leading candidate. This computational study will guide experimental validation and structure-based optimization of next-generation SOD3 inhibitors for blood cancer.

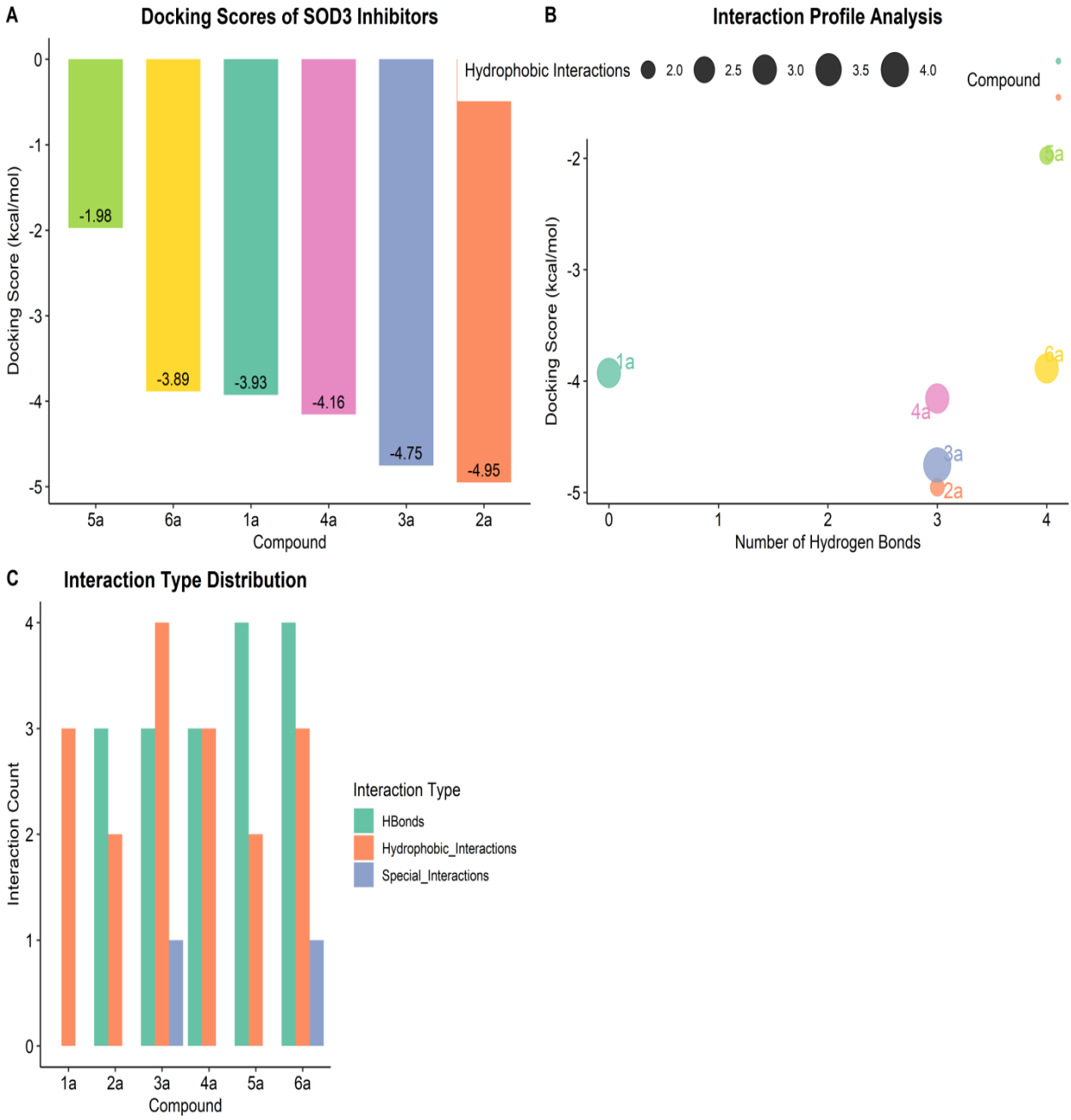

Figure 4.10: Docking score of SOD3 inhibitor

The human SOD3 structure (PDB ID: 4M0Z), an antioxidant enzyme, demonstrates potential anti-blood cancer activity by mitigating oxidative stress in hematological malignancies.

Frontier in Medical & Health Research

ISSN: (e) 3007-1607 (p) 3007-1593

Table 4.11: Molecular Docking Scores of Selected bio-molecules (1a-6a) against the anti-blood cancer enzyme SOD3 (PDB ID: 4M0Z)

Selected bio-molecules	Docking score (Ref/selected bio-molecules)	H-Bond Interactions	Nature of interactions
1a	-3.927	1	1. Pi-Alkyl
2a	-4.953	2	1. Conventional Hydrogen Bond 2. Carbon Hydrogen Bond 3. Pi-Alkyl
3a	-4.754	1	1. Conventional Hydrogen Bond 2. Pi-Pi T-shaped 3. Pi-Alkyl
4a	-4.157	2	1.Conventional Hydrogen Bond 2.Carbon Hydrogen Bond 3. Pi-Alkyl
5a	-1.975	2	1.Conventional Hydrogen Bond 2.Carbon Hydrogen Bond 3. Pi-Alkyl 4. Alkyl
6a	-3.887	2	1.Conventional Hydrogen Bond 2.Carbon Hydrogen Bond 3. Pi-Alkyl 4. Alkyl

Table 4.12: Molecular Docking features of selected bio-molecules (1a-6a) against the anti-blood cancer enzyme SOD3 (PDB ID: 4M0Z)

Selected bio-molecules	Amino acids on active sites with	Binding Mode Features
1a	ALA389, LEU489,ILE369	Form strong Pi-Alkyl with active site residues.
2a	LEU489, ILE369, ASP500, ASN487, MET438, ALA389	Forms three strong H-bonds and Pi-Alkyl with active site residues.
3a	CYS442, VAL377, LEU489, ALA389 ILE369, MET438, PHE437	Forms three strong H-bonds, Pi-Pi T-shaped and Pi-Alkyl with active site residues.
4a	ILE369, GLU436, ALA389, MET438 LEU489, CYS442, GLY441	Forms three strong H-bonds and Pi-Alkyl with active site residues.
5a	MET438, LEU489, ALA389, GLU436, VAL377	Forms four strong H-bonds, Alkyl and Pi-Alkyl with active site residues.
6a	ALA389, LEU489, LYS391, ARG486 GLY441, CYS442	Forms four strong H-bonds, Alkyl and Pi-Alkyl with active site residues.

Molecular Docking of **1a** with **SOD3 (PDB ID: 4M0Z)**, an antioxidant enzyme, demonstrates potential anti-blood cancer activity by mitigating oxidative stress in hematological malignancies**.**

Volume 4, Issue 3, 2026

Frontier in Medical & Health Research

ISSN: (e) 3007-1607 (p) 3007-1593

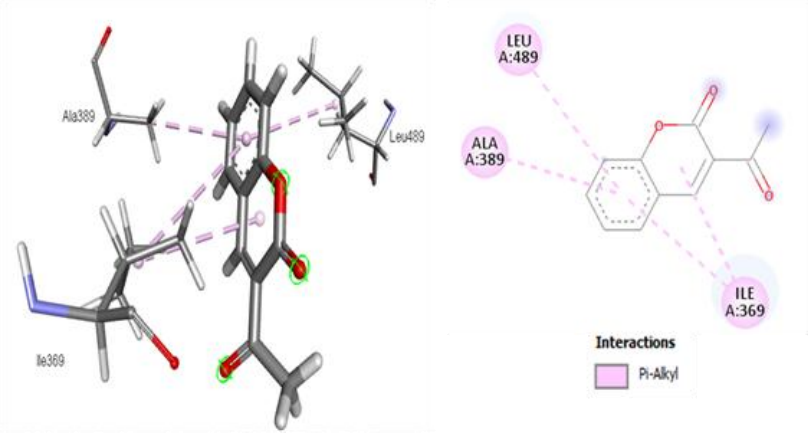

Figure 4.11: Molecular docking of 1a withSOD3

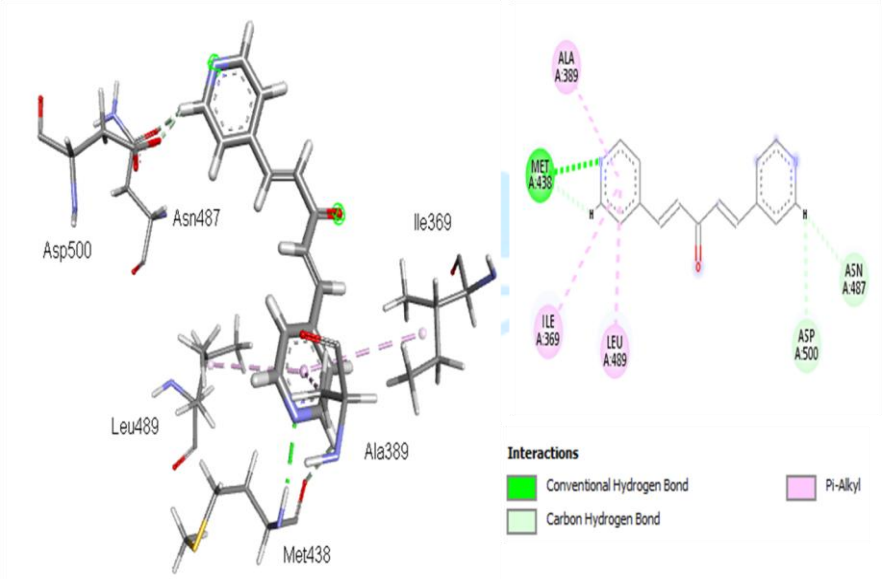

Figure 4.12: Molecular docking of **2a** with **SOD3 (PDB ID: 4M0Z)**

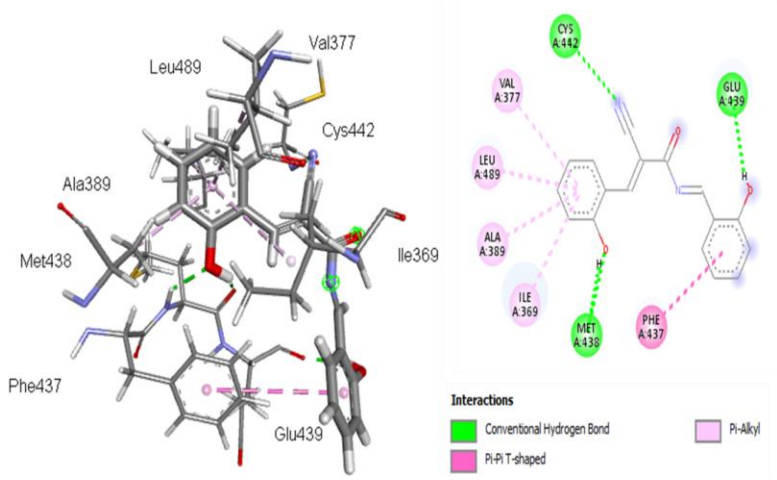

Figure 4.13: Molecular docking of **3a** withSOD3

Molecular Docking of **3a** with **SOD3 (PDB ID: 4M0Z)**, an antioxidant enzyme, demonstrates potential anti-blood cancer activity by mitigating oxidative stress in hematological malignancies**.**

Volume 4, Issue 3, 2026

Frontier in Medical & Health Research

ISSN: (e) 3007-1607 (p) 3007-1593

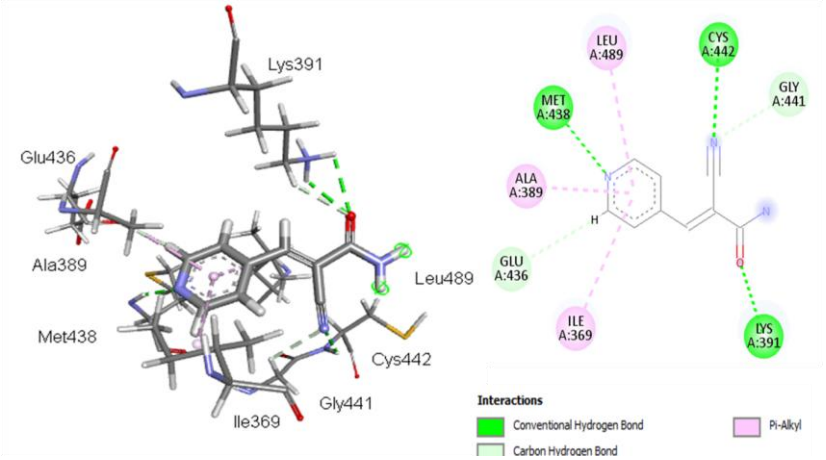

Figure 4.14: Molecular docking of **4a** withSOD3

Molecular Docking of **4a** with **SOD3 (PDB ID: 4M0Z)**, an antioxidant enzyme, demonstrates potential anti-blood cancer activity by mitigating oxidative stress in hematological malignancies**.**

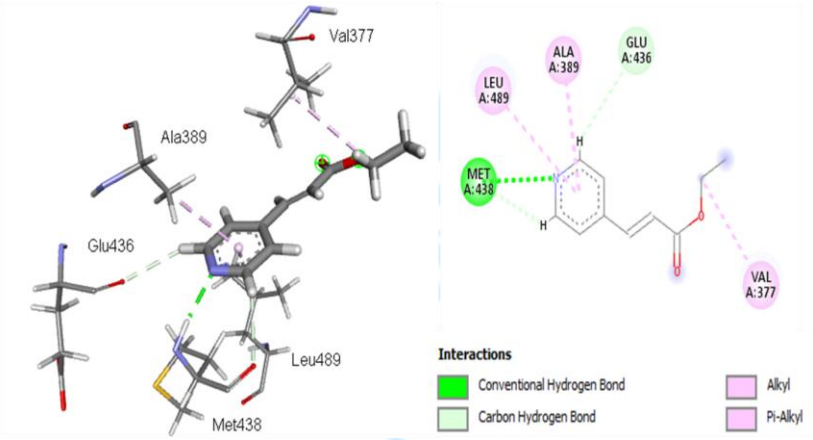

Molecular Docking of **5a** with **SOD3 (PDB ID: 4M0Z)**, an antioxidant enzyme, demonstrates potential anti-blood cancer activity by mitigating oxidative stress in hematological malignancies**.**

Figure 4.15: Molecular docking of **5a** withSOD3

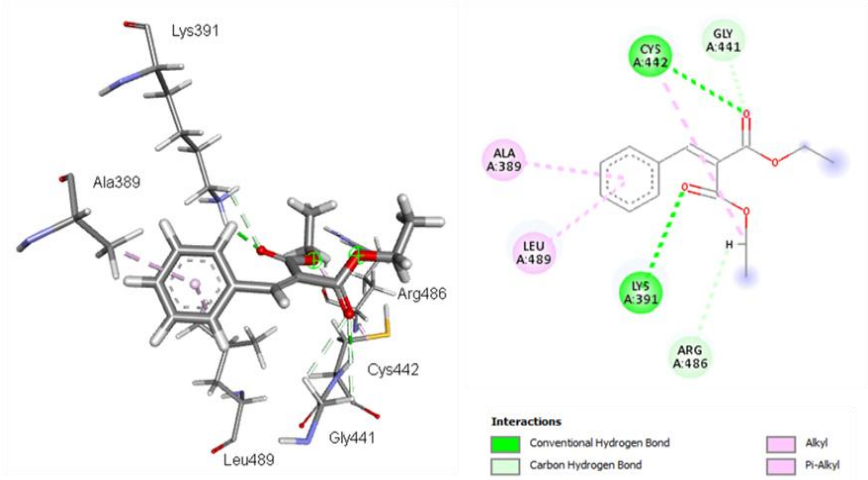

Molecular Docking of **6a** with **SOD3 (PDB ID: 4M0Z)**, an antioxidant enzyme, demonstrates potential anti-blood cancer activity by mitigating oxidative stress in hematological malignancies**.**

Figure 4.16: Molecular docking of **6a** with SOD3

Frontier in Medical & Health Research
ISSN: (e) 3007-1607 (p) 3007-1593

5. CONCLUSION

This study suggests that triethylamine (TEA) as a base may produce high Knoevenagel derivatives under moderate and effective conditions. After spectroscopy confirmed compound structures, computational and biological profiles were examined. Screening revealed that some derivatives had potent zones of inhibition against certain infections and others showed promise as antifungal and antibacterial agents. The findings support Knoevenagel compounds as multi-bacteria antimicrobials. To study anticancer effects, molecular docking targeted blood cancer proteins. New chemicals stick to protein active sites. These compounds' effects on blood cancer cell lines suggest treatment efficacy. In this experiment, lab and computer results matched. All steps for developing, analyzing, and synthesizing novel Knoevenagel derivatives are covered. Scientists can develop antibacterial and anticancer compounds using biological screening and molecular docking. The findings must be confirmed in vitro, in vivo, and mechanistic studies before these compounds can enter clinical trials. Computational research has made three major contributions to hematological malignancies SOD3 inhibitors. A balanced interaction profile of polar contacts with catalytic residues (ASP500, ASN487) and hydrophobic packing in the conserved subpocket (ALA389, LEU489, ILE369) and superior binding affinity (-4.953 kcal/mol) made compound 2a the most promising. Compound 5a failed despite its hydrogen bonding potential, demonstrating that effective inhibitors must engage both the catalytic triad and hydrophobic regions while maintaining steric compatibility. Third, we found competitive, allosteric, and redox modulation inhibition mechanisms that offer multiple therapeutic approaches. These findings are timely given the growing recognition of SOD3's role in hematological malignancies and the need for targeted oxidative stress modulators. These computational findings rationalize medicinal chemistry optimization, including hydrogen bonding network enhancement, hydrophobic contact optimization, and strategic aromatic moieties. Experimental verification is needed. This study shows that the knoevenagel scaffold can be used to develop novel redox-modulating therapeutics, with compound 2a as a good preclinical basis. These predictions should be validated in vitro and structure-based optimized using this study's principles to advance SOD3-targeted blood cancer therapy clinical translation.

6. REFERENCES

Ali, I., et al., *Heterocyclic scaffolds: centrality in anticancer drug development.* Current drug targets, 2015. **16**(7): p. 711-734.

Rupainwar, R. and J. Pandey, *The importance and applications of knoevenagel reaction (brief review).* Oriental Journal of Chemistry, 2019. **35**(1): p. 423.

van Beurden, K., et al., *The Knoevenagel reaction: a review of the unfinished treasure map to forming carbon–carbon bonds.* Green chemistry letters and reviews, 2020. **13**(4): p. 349-364.

Tokala, R., D. Bora, and N. Shankaraiah, *Contribution of Knoevenagel condensation products toward the development of anticancer agents: An updated review.* ChemMedChem, 2022. **17**(8): p. e202100736.

Deshmukh, M., et al., *Green approach for Knoevenagel condensation of aromatic aldehydes with active methylene group.* Synthetic Communications, 2012. **42**(8): p. 1177-1183.

Abdella, A.M., et al., *Synthesis of heterocyclic compounds via Michael and Hantzsch reactions.* Journal of Heterocyclic Chemistry, 2020. **57**(4): p. 1476-1523.

Menegatti, R., *Green chemistry–aspects for the Knoevenagel reaction*, in *Green chemistry-environmentally benign approaches*. 2012, IntechOpen.

Boumendjel, A., J.-M. Nuzillard, and G. Massiot, *Synthesis of ajmalicine derivatives using Wittig-Horner and Knoevenagel reactions.* Tetrahedron letters, 1999. **40**(51): p. 9033-9036.

Lau, W., K.L. Yeung, and R. Martin-Aranda, *Knoevenagel condensation reaction between* benzaldehyde *and ethyl acetoacetate in microreactor and membrane microreactor.* Microporous and mesoporous materials, 2008. **115**(1-2): p. 156-163.

Anastas, P.T. and J.C. Warner, *Green chemistry: theory and practice*. 2000: Oxford university press.

Texier-Boullet, F. and A. Foucaud, *Knoevenagel condensation catalysed by aluminium oxide.*

Frontier in Medical & Health Research

ISSN: (e) 3007-1607 (p) 3007-1593

Tetrahedron Letters, 1982. **23**(47): p. 4927-4928.

Chanda, A. and V.V. Fokin, *Organic synthesis "on water"*. Chemical reviews, 2009. **109**(2): p. 725-748.

Cabello, J.A., et al., *Knoevenagel condensation in the heterogeneous phase using aluminum phosphate-aluminum oxide as a new catalyst.* The Journal of Organic Chemistry, 1984. **49**(26): p. 5195-5197.

Mallouk, S., et al., *Microwave-assisted and efficient solvent-free knoevenagel condensation. A sustainable protocol using porous calcium hydroxyapatite as catalyst.* Molecules, 2010. **15**(2): p. 813-823.

Badiger, K.B. and K. Kamanna, *Knoevenagel condensation reaction catalysed by agro-waste extract as a greener solvent catalyst.* Organic Communications, 2021. **14**(1): p. 81-91.

Zhao, X.-L., et al., *Polyguanidine as a highly efficient and reusable catalyst for knoevenagel condensation reactions in water.* Australian Journal of Chemistry, 2013. **66**(4): p. 500-504.

Wang, D.-Y., et al., *Condensation reactions of aromatic aldehydes with active methylene compounds catalyzed by alkaline ionic liquid.* Synthetic Communications, 2011. **41**(20): p. 3060-3065.

Xu, B., et al., *Polyoxomolybdates as efficient catalysts for Knoevenagel condensation reaction of benzaldehyde and ethyl cyanoacetate under mild condition.* Journal of Materials Science, 2021. **56**: p. 4654-4665.

Sakthivel, B. and A. Dhakshinamoorthy, *Chitosan as a reusable solid base catalyst for Knoevenagel condensation reaction.* Journal of Colloid and Interface Science, 2017. **485**: p. 75-80.

Vekariya, R.H. and H.D. Patel, *Recent advances in the synthesis of coumarin derivatives via Knoevenagel condensation: A review.* Synthetic Communications, 2014. **44**(19): p. 2756-2788.

Jimenez, D.E., et al., *Green synthetic methodology of (E)-2-cyano-3-aryl selective knoevenagel adducts under microwave irradiation.* Current Microwave Chemistry, 2019. **6**(1): p. 54-60.

Almuzaini, H., *Deep eutectic solvents (DES) as catalyst and solvent for Knoevenagel condensation reactions*. 2015, Middle Tennessee State University.

Mohareb, R.M., N.N. El-Sayed, and M.A. Abdelaziz, *The Knoevenagel reactions of pregnenolone with cyanomethylene reagents: Synthesis of thiophene, thieno [2, 3-b] pyridine, thieno [3, 2-d] isoxazole derivatives of pregnenolone and their in vitro cytotoxicity towards tumor and normal cell lines.* Steroids, 2013. **78**(12-13): p. 1209-1219.

Koohi, F., et al., *Leukemia in Iran: epidemiology and morphology trends.* Asian Pacific Journal of Cancer Prevention, 2015. **16**(17): p. 7759-7763.

Paul, S., et al., *Acentric Order–Disorder Zn3Sb4CO6F6: Crystal Structure, Dye Degradation, Cr (VI) Removal, Antibacterial Activity, and Catalytic C–C Bond Formation.* Inorganic Chemistry, 2025.

Tavakoli, S. and A. Abbasi, *Bimetallic Co-Mg MOF: an efficient heterogeneous catalyst for room-temperature Knoevenagel condensation.* Research on Chemical Intermediates, 2025: p. 1-16.

Cardoso, B.S., et al., *Synthesis, Biological Evaluation and Principal Component Analysis of Arylidene Analogues of Barbituric Acid Obtained via Knoevenagel Condensation.* Journal of the Brazilian Chemical Society, 2025. **36**(7): p. e-20250057.

Nguyen, T.C., et al., *Synthesis, evaluation of α-glucosidase inhibitory and antimicrobial activities of novel N-(5-arylidene-4-oxo-2-thioxothiazolidin-3-yl)-2-(naphthalen-1-yl) acetamide derivatives.* Journal of Molecular Structure, 2025. **1326**: p. 141068.

Nampally, U., et al., *Facile synthesis of substituted 2-styrylnaphthyridine derivatives via sp3 CH functionalization under mild conditions and their antimicrobial activity and Electrochemical properties.* Journal of Molecular Structure, 2025. **1324**: p. 140604.

Killi, N., K. Rumpke, and D. Kuckling, *Synthesis of Curcumin Derivatives via Knoevenagel Reaction Within a Continuously Driven Microfluidic Reactor Using Polymeric Networks Containing Piperidine as a Catalyst.* Gels, 2025. **11**(4): p. 278.

Ingale, N., et al., *Synthesis and evaluation of anti-inflammatory and analgesic activity of 3-[(5-substituted-1, 3, 4-oxadiazol-2-yl-thio) acetyl]-*

Frontier in Medical & Health Research

ISSN: (e) 3007-1607 (p) 3007-1593

2H-chromen-2-ones. Medicinal Chemistry Research, 2012. **21**: p. 16-26.

Gomaa, H.A., et al., *Design, synthesis, and biological investigation of new thiazole-based derivatives as multi-targeted inhibitors endowed with antiproliferative, antioxidant, and antibacterial properties*. Frontiers in Chemistry, 2025. **13**: p. 1595997.

Badiger, K.B. and K. Kamanna, *Microwave-accelerated Eco-friendly Performance of the Knoevenagel Condensation Reaction with Various Active Methylene Derivat-ives evaluation of Electrochemical Properties*. Current Organocatalysis, 2023. **10**(2): p. 113-127.

van Schijndel, J., et al., *The green Knoevenagel condensation: solvent-free condensation of benzaldehydes*. Green Chemistry Letters and Reviews, 2017. **10**(4): p. 404-411.

Tietze, L.F. and N. Rackelmann, *Domino reactions in the synthesis of heterocyclic natural products and analogs*. Pure and Applied Chemistry, 2004. **76**(11): p. 1967-1983.

Jadhav, A.L. and G.D. Yadav, *Clean synthesis of benzylidenemalononitrile by Knoevenagel condensation of benzaldehyde and malononitrile: effect of combustion fuel on activity and selectivity of Ti-hydrotalcite and Zn-hydrotalcite catalysts*. Journal of Chemical Sciences, 2019. **131**: p. 1-14.

Ashokkumar, V., A. Siva, and B. Sankar, *The organocatalytic highly enantioselective Knoevenagel condensation: applications in the synthesis of various chiral amide derivatives*. Journal of the Iranian Chemical Society, 2019. **16**: p. 1939-1955.

Rauf, A., et al., *Synthesis of novel cyanoacetamides derivatives and their urease inhibition studies*. European Journal of Chemistry, 2015. **6**(2): p. 163-168.

McNulty, J., J.A. Steere, and S. Wolf, *The ultrasound promoted Knoevenagel condensation of aromatic aldehydes*. Tetrahedron Letters, 1998. **39**(44): p. 8013-8016.

Mondal, J., A. Modak, and A. Bhaumik, *Highly efficient mesoporous base catalyzed Knoevenagel condensation of different aromatic aldehydes with malononitrile and subsequent noncatalytic Diels–Alder reactions*. Journal of Molecular Catalysis A: Chemical, 2011. **335**(1-2): p. 236-241.

Salem, M.A., et al., *Novel 3-Substituted-2H-Chromene Scaffold Based Fluorinated Hydrophobic Fragment as In-Vitro Antiproliferative Agents and Apoptosis Inducers Targeting Both VEGFR-2/BRAFV600E and h-DHFR With Molecular Docking Simulation*. Drug Development Research, 2025. **86**(2): p. e70085.

Retnosari, R., et al. *The antibacterial activity of vanillin derivative compounds*. in *AIP Conference Proceedings*. 2021. AIP Publishing.

Mannarsamy, M. and G. Prabusankar, *Highly active copper (I)-chalcogenone catalyzed Knoevenagel condensation reaction using various aldehydes and active methylene compounds*. Catalysis Letters, 2022: p. 1-6.

Dehghani, P., D. Elhamifar, and S. Kargar, *Amine functionalized magnetic resorcinol formaldehyde as a green and reusable nanocatalyst for the Knoevenagel condensation*. Scientific Reports, 2025. **15**(1): p. 2873.

Louzada, L.D.T., P.N. Batalha, and F.B. de Almeida, *Coordination Polymers As Catalysts in Knoevenagel Condensations— A Critical Review Analysis under Synthesis Conditions and Green Chemistry*. Crystal Growth & Design, 2025.

Snigdha, K., et al., *Green synthesis of pyrazole derivatives via one-pot three component Knoevenagel–Michael addition utilizing TiO2/RuO2/CuO as a ternary nanocatalytic system: characterization, DFT and molecular docking studies*. Research on Chemical Intermediates, 2025: p. 1-27.

Seto, H., et al., *Polymer microgel particles as basic catalysts for Knoevenagel condensation in water*. Polymer Journal, 2016. **48**(8): p. 897-904.

Trotzki, R., M.M. Hoffmann, and B. Ondruschka, *The Knoevenagel condensation at room temperature*. Green Chemistry, 2008. **10**(8): p. 873-878.

Rocha, K.L.A., et al., *Synthesis, characterization and functionalization of MOFs and their use in Knoevenagel condensation reactions between ethyl cyanoacetate and 4-nitrobenzaldehyde*. Brazilian Journal of Chemical Engineering, 2024: p. 1-13.

Frontier in Medical & Health Research

ISSN: (e) 3007-1607 (p) 3007-1593

Parida, K.M. and D. Rath, *Amine functionalized MCM-41: An active and reusable catalyst for Knoevenagel condensation reaction.* Journal of Molecular Catalysis A: Chemical, 2009. **310**(1-2): p. 93-100.

Wang, J.-J., X. Cheng, and C.-H. Zhang, *Sturcture, characterization and computation of 1, 1'-dibenzyl-[4, 4'-bipyridine]-1, 1'-diium nitrate.* Bulletin of the Chemical Society of Ethiopia, 2025. **39**(5): p. 987-1000.

Anbu, N., et al., *Chitosan as a biodegradable heterogeneous catalyst for Knoevenagel condensation between benzaldehydes and cyanoacetamide.* Catalysis Communications, 2020. **138**: p. 105954.

Xu, J., et al., *Synthesis of three-dimensional mesostructured graphitic carbon nitride materials and their application as heterogeneous catalysts for Knoevenagel condensation reactions.* Catalysis letters, 2013. **143**: p. 600-609.

Panja, S.K., N. Dwivedi, and S. Saha, *First report of the application of simple molecular complexes as organo-catalysts for Knoevenagel condensation.* RSC Advances, 2015. **5**(80): p. 65526-65531.

Rao, P.S. and R. Venkataratnam, *Zinc chloride as a new catalyst for Knoevenagel condensation.* Tetrahedron letters, 1991. **32**(41): p. 5821-5822.

Ono, Y., *Solid base catalysts for the synthesis of fine chemicals.* Journal of Catalysis, 2003. **216**(1-2): p. 406-415.

Jyothi, T., et al., *Selective O-methylation of catechol using dimethyl carbonate over calcined Mg–Al hydrotalcites.* Applied catalysis A: general, 2001. **211**(1): p. 41-46.

Deshmukh, G.P. and G.D. Yadav, *Facile synthesis of dicamba ester over heterogeneous magnesium oxide and kinetic modelling.* Chemical Engineering Journal, 2017. **309**: p. 663-673.

Mashelkar, R., *Solid state chemistry: selected papers of CNR Rao*. Vol. 4. 1995: World Scientific.

Patil, K.C., S.T. Aruna, and S. Ekambaram, *Combustion synthesis.* Current opinion in solid state and materials science, 1997. **2**(2): p. 158-165.

Abed, H.H., et al. *Synthesis and evaluation of chalcone derivatives for antimicrobial and antioxidant activities using microwave-assisted methodology*. in *AIP Conference Proceedings*. 2025. AIP Publishing.

Luo, H., et al., *Aerobic oxidative cleavage of 1, 2-diols catalyzed by atomic-scale cobalt-based heterogeneous catalyst.* Communications Chemistry, 2019. **2**(1): p. 17.

Yoshida, A., S. Hikichi, and N. Mizuno, *Acid–base catalyses by dimeric disilicoicosatungstates and divacant γ-Keggin-type silicodecatungstate parent: Reactivity of the polyoxometalate compounds controlled by step-by-step protonation of lacunary WO sites.* Journal of organometallic chemistry, 2007. **692**(1-3): p. 455-459.

Hayashi, S., et al., *Application of group V polyoxometalate as an efficient base catalyst: a case study of decaniobate clusters.* RSC Advances, 2016. **6**(20): p. 16239-16242.

Szegner, J., K.L. Yeung, and A. Varma, *Effect of catalyst distribution in a membrane reactor: experiments and model.* AIChE journal, 1997. **43**(8): p. 2059-2072.

Lai, S.M., R. Martin-Aranda, and K.L. Yeung, *Knoevenagel condensation reaction in a membrane microreactor.* Chemical communications, 2003(2): p. 218-219.

Zhang, X., et al., *An investigation of Knoevenagel condensation reaction in microreactors using a new zeolite catalyst.* Applied Catalysis A: General, 2004. **261**(1): p. 109-118.

Pattabiraman, V.R. and J.W. Bode, *Rethinking amide bond synthesis.* Nature, 2011. **480**(7378): p. 471-479.

Choudary, B., et al., *Knoevenagel and aldol condensations catalysed by a new diamino-functionalised mesoporous material.* Journal of Molecular Catalysis A: Chemical, 1999. **142**(3): p. 361-365.

Tandel, P., et al., *Investigation of recent advancement in the pharmacological potential of C-3 substituted coumarin derivatives against S. aureus.* Discover Chemistry, 2025. **2**(1): p. 58.

Kugita, T., et al., *Mesoporous Al-containing MCM-41 molecular sieves: highly active catalysts for Diels–Alder reaction of cyclopentadiene with α, β-unsaturated aldehydes.* Applied Catalysis A: General, 2003. **245**(2): p. 353-362.

Zukić, S., et al., *Antioxidant, Antimicrobial and Antiproliferative Activities of Synthesized 2, 2, 5, 5-Tetramethyl-9-aryl-3, 4, 5, 6, 7, 9-*

Frontier in Medical & Health Research

ISSN: (e) 3007-1607 (p) 3007-1593

hexahydro-1H-xanthene-1, 8 (2H)-dione Derivatives. Croatica chemica acta, 2018. **91**(1): p. 1-9.

Yadav, R., D. Saini, and D. Yadav, *Synthesis and evaluation of vanillin derivatives as antimicrobial agents.* Turk J Pharm Sci, 2018. **15**(1): p. 57-62.

Zhou, Z. and X. Deng, *[Et3NH][HSO4] catalyzed efficient and green synthesis of 1, 8-dioxo-octahydroxanthenes.* Journal of Molecular Catalysis A: Chemical, 2013. **367**: p. 99-102.

Verma, G.K., et al., *An efficient one-pot solvent-free synthesis and photophysical properties of 9-aryl/alkyl-octahydroxanthene-1, 8-diones.* Tetrahedron, 2011. **67**(20): p. 3698-3704.

Alvarado, E., et al., *N-Heterocyclic Carbenes and Imidazole-2-thiones as Ligands for the Gold (I)-Catalysed Hydroamination of Phenylacetylene.* Chemistry–A European Journal, 2012. **18**(38): p. 12112-12121.

Maruthupandi, M. and G. Prabusankar, *Catalytically active coordination polymer with a tiny Zn 2 Se 2 ring bridged by bis-selone.* RSC advances, 2020. **10**(48): p. 28950-28957.

Abbott, A.P., et al., *Novel solvent properties of choline chloride/urea mixtures.* Chemical communications, 2003(1): p. 70-71.

Datta, S., *Antimicrobial Analysis of extracts of rhizomes of hedychium Spicatum in A. Rees of Himachal Pradesh.* IJSAT-International Journal on Science and Technology. **16**(2).

Ruß, C. and B. König, *Low melting mixtures in organic synthesis–an alternative to ionic liquids?* Green Chemistry, 2012. **14**(11): p. 2969-2982.

Abbott, A.P., et al., *Ionic liquids based upon metal halide/substituted quaternary ammonium salt mixtures.* Inorganic chemistry, 2004. **43**(11): p. 3447-3452.

Hayyan, A., et al., *Fruit sugar-based deep eutectic solvents and their physical properties.* Thermochimica Acta, 2012. **541**: p. 70-75.

Handy, S., *Deep eutectic solvents in organic synthesis.* Ionic Liquids-Current State of the Art, 2015: p. 59-92.

Singh, B., H. Lobo, and G. Shankarling, *Selective N-alkylation of aromatic primary amines catalyzed by bio-catalyst or deep eutectic solvent.* Catalysis letters, 2011. **141**: p. 178-182.

Liu, S., et al., *Choline chloride and urea based eutectic solvents: effective catalytic systems for the Knoevenagel condensation reactions of substituted acetonitriles.* Journal of Chemical Research, 2014. **38**(3): p. 186-188.

Nuha, D., et al., *Development and Biological Assessment of Thiazole-Based Pyridines for Targeted Therapy in Lung Cancer.* ACS omega, 2025.

Keshavarzipour, F. and H. Tavakol, *The synthesis of coumarin derivatives using choline chloride/zinc chloride as a deep eutectic solvent.* Journal of the Iranian Chemical Society, 2016. **13**: p. 149-153.

Yarovenko, V., et al., *Synthesis of 2-thioxo-1, 3-thiazolidin-4-one derivatives.* Russian Chemical Bulletin, 2007. **56**(8): p. 1624-1630.

Suresh and J.S. Sandhu, *Ultrasound-assisted synthesis of 2, 4-thiazolidinedione and rhodanine derivatives catalyzed by task-specific ionic liquid:[TMG][Lac].* Organic and medicinal chemistry letters, 2013. **3**: p. 1-6.

Li, J. and Q. Pang, *Oxidative stress-associated protein tyrosine kinases and phosphatases in Fanconi anemia.* Antioxidants & Redox Signaling, 2014. **20**(14): p. 2290-2301.

Molnar, M., et al., *Environmentally friendly approach to Knoevenagel condensation of rhodanine in choline chloride: Urea deep eutectic solvent and QSAR studies on their antioxidant activity.* Molecules, 2018. **23**(8): p. 1897.

Birolli, W.G., et al., *Synthesis of Knoevenagel adducts under microwave irradiation and biocatalytic ene-reduction by the marine-derived fungus Cladosporium sp. CBMAI 1237 for the production of 2-cyano-3-phenylpropanamide derivatives.* Marine Biotechnology, 2020. **22**: p. 317-330.

Abulkhair, H.S. and K. El-Adl, *A decade of research effort in synthesis, biological activity assessments, and mechanistic investigations of sulfamethazine-incorporating molecules.* Archiv der Pharmazie, 2025. **358**(3): p. e2500033.

Frontier in Medical & Health Research

ISSN: (e) 3007-1607 (p) 3007-1593

Kearon, C., et al., *Antithrombotic therapy for VTE disease: CHEST guideline and expert panel report.* Chest, 2016. **149**(2): p. 315-352.

Erythropel, H.C., et al., *The Green ChemisTREE: 20 years after taking root with the 12 principles.* Green chemistry, 2018. **20**(9): p. 1929-1961.

Bergbreiter, D.E., *Soluble polymers as tools in catalysis*. 2014, ACS Publications.

Wang, G., et al., *Gel catalysts that switch on and off.* Proceedings of the National Academy of Sciences, 2000. **97**(18): p. 9861-9864.

Wang, S., et al., *The Knoevenagel condensation of aromatic aldehydes with malononitrile or ethyl cyanoacetate in the presence of CTMAB in water.* Synthetic Communications, 2001. **31**(5): p. 673-677.

Zhu, Y.-Z., et al., *Synergistic antifungal activity of minocycline as an effective augmenting agent of fluconazole against drug-resistant Candida tropicalis.* Microbiology Spectrum, 2025: p. e03185-24.

Dyachenko, V., et al., *Knoevenagel Reactions of Indole-3-carbaldehyde. Synthesis of 3-Substituted Indole Derivatives.* Russian Journal of Organic Chemistry, 2018. **54**: p. 1777-1784.